

Contents

6.0	SSC Database: Earthquake Catalog.....	6.1
6.1	Catalog Region and Parameter Limits.....	6.1
6.1.1	Geographic Extent.....	6.1
6.1.2	Magnitude Cut-Off.....	6.2
6.1.3	Types of Earthquakes Investigated.....	6.2
6.1.4	Time Span Covered.....	6.4
6.2	Earthquake Data Sources.....	6.4
6.2.1	Historical Seismicity.....	6.4
6.2.2	Regional-Scale Catalogs.....	6.5
6.2.3	Continental-Scale Catalogs.....	6.6
6.2.4	Previous Catalog Compilation Efforts.....	6.7
6.2.5	Identification of Unique Earthquake Entries.....	6.7
6.3	Epicentral Locations.....	6.8
6.4	Focal Depth.....	6.12
6.4.1	Routine Location Procedure and Depth Determination.....	6.12
6.4.2	Spatial Variation of Depth Distribution Across Study Region.....	6.12
6.5	Magnitude Homogenization.....	6.14
6.5.1	Target Magnitude and Available Magnitudes.....	6.15
6.5.2	Conversion from M_C , M_D , and Other Magnitude Scales.....	6.16
6.5.3	Conversion from Macroseismic Intensities.....	6.25
6.5.4	Treatment of Magnitude Uncertainties in Recurrence Calculations.....	6.28
6.5.5	Uniform Moment Magnitude Catalog of $E[M]$ and N^* Values.....	6.29
6.6	Declustering of the Earthquake Catalogs.....	6.33
6.6.1	Alternative Declustering Approaches.....	6.33
6.6.2	Application to Hanford PSHA Project Catalog.....	6.34
6.7	Catalog Completeness.....	6.36
6.7.1	The Stepp Method.....	6.36
6.7.2	Probability of Detection in Space and Time.....	6.37
6.8	References.....	6.39

Figures

6.1	Schematic explaining the criteria for assigning earthquakes to the slab.....	6.3
6.2	Map of the regional distribution of catalogs used to compile the crustal and subduction catalogs.	6.5
6.3	Distribution of seismicity in the area covered by the crustal earthquake catalog.....	6.9
6.4	Distribution of seismicity in the area covered by the subduction earthquake catalog.....	6.10
6.5	Map of earthquake epicenters recorded during the pre-, early, and modern instrumental periods.....	6.11
6.6	Map showing the cross-section location, cross section at -120.5°E , cross section at -119.5°E , cross section at 47.5°N , and cross section at 46.5°N	6.13
6.7	Cross section drawn along the transect shown in panel (a); panel (b) shows hypocenters along the transect from subduction catalog	6.14
6.8	Relationship between m_b and M by region and source.	6.18
6.9	Regression of m_b and M	6.19
6.10	Relationship between M_S and M by region and M_S type and source.....	6.20
6.11	Regression of M_S and M	6.21
6.12	Relationship of M_C and M_D	6.22
6.13	Regression of M_C and $M_D - M$	6.23
6.14	Regression of M_L and M	6.24
6.15	Regression of M_L and M_D	6.25
6.16	Relationships between I_0 vs M ; I_0 vs M_D ; I_0 vs M_S	6.26
6.17	Regression between I_0 and M	6.27
6.18	Map of the crustal earthquake catalog with magnitudes given in $E[M]$	6.30
6.19	Map of the subduction earthquake catalog in $E[M]$	6.31
6.20	Map of the subduction earthquake catalog in $E[M]$ including earthquakes with unknown depths.....	6.32

Tables

6.1	Magnitude types and magnitude ranges in the crustal earthquake catalog.	6.15
6.2	Magnitude types and magnitude ranges in the subduction earthquake catalog.	6.15
6.3	Number of earthquakes per magnitude bin from the declustered crustal catalogs and the declustered subduction catalogs.....	6.35
6.4	P^D and equivalent time of completeness by completeness region, magnitude and time intervals, and catalog.	6.38

6.0 SSC Database: Earthquake Catalog

This chapter describes the compilation of the two earthquake catalogs used for the Hanford PSHA project. Hazard sensitivity analysis presented at Workshop 1 (V. Montaldo-Falero) indicated that the seismic hazard at the Hanford Site comes from local crustal sources and from distant sources associated with the Cascadia subduction. These two types of earthquakes have different characteristics and for the purpose of calculating earthquake recurrence parameters need to be maintained in two separate catalogs. Details about the geographic and temporal extent of the two catalogs are given in Section 6.1. The process of compiling the two earthquake catalogs (Section 6.2) follows the example of NUREG-2115 (NRC 2012) for the central and eastern United States, where records (i.e., earthquake catalog entries) from multiple sources were merged, compared, and uniformly processed to obtain a complete catalog with a uniform size measure for all earthquakes. As discussed in NUREG-2115, the purpose of merging earthquake records from different sources is to limit the effect of partial network coverage in time and space, and to obtain a data set of alternative magnitude measures for use in deriving magnitude conversion equations. Sections 6.3 and 6.4 discuss the spatial distribution of earthquakes and their depths. This discussion supplements the discussions of the tectonic interpretations of the seismicity data that are given in Section 4.4. Section 6.5 describes the process of homogenizing the magnitudes to a uniform moment magnitude measure and the calculation of unbiased earthquake counts to be used in recurrence analysis. This is done by following the procedure developed in NUREG-2115 that allows proper treatment of the uncertainty in the magnitude estimates and in the magnitude conversions. The last two sections describe the declustering process used to remove all foreshocks and aftershocks (Section 6.6), and the assessment of the completeness of the catalogs as a function of location, time, and earthquake size (Section 6.7). These analyses of the earthquake catalog provide a basis for calculating earthquake recurrence parameters, which is discussed in Section 8.3.2.8.

6.1 Catalog Region and Parameter Limits

The geographic extent and the criteria used to compile the crustal and subduction earthquake catalogs are presented in this section. Crustal earthquakes are generated by sources within the region surrounding the Hanford Site. The limits of this region are described in Section 6.1.1. Subduction earthquakes associated with the Cascadia subduction zone are located to the west of the site and at depths greater than crustal sources.

6.1.1 Geographic Extent

The Hanford crustal earthquake catalog covers the region between latitude 45°N and 49°N and longitude -121.5°E and -117.5°E. The extent of the region is sufficient to cover the primary sources of seismicity around the Hanford Site, namely the Yakima Fold Belt (YFB) to the south and the epicentral area of the Lake Chelan earthquake to the north.

Earthquakes associated with the Cascadia subduction zone are selected between latitude 43°N and 50°N, and west of longitude -120°E. This area includes the coastal regions of Oregon, Washington, and portions of British Columbia, and extends east to include the Cascade Mountains. Both crustal and subduction earthquakes occur within this region; the two types of seismicity are separated based on the location of their hypocenters with respect to the depth of the top of the slab, as modeled by McCrory et al. (2006). Section 6.1.3 describes this process in more detail.

6.1.2 Magnitude Cut-Off

The approach to calculating a uniform magnitude followed for this project is the same as that described by the NRC in NUREG-2115 and by the Electric Power Research Institute Seismic Owners Group (EPRI-SOG 1988), in which the uncertainty in the magnitude is accounted for through a variance-weighted estimate of the expected value of the true moment magnitude ($E[M]$). To correctly incorporate the uncertainty, it is important to collect all possible magnitude estimates for each earthquake; this is achieved by using multiple sources of earthquake records such as online earthquake catalogs from various agencies and published literature. In all web-based searches for earthquakes the magnitude type and magnitude range fields were left undefined so that all possible values would be retrieved. However, because of the range of applicability of the magnitude conversion relations used to calculate $E[M]$, the minimum magnitude in the earthquake catalogs is $E[M] 1.85$.

6.1.3 Types of Earthquakes Investigated

The earthquake catalogs are compiled by merging records from different sources, and it is anticipated that in this process some records of non-tectonic events may also be included. These records need to be identified because they should not be used in the hazard analysis. This task is particularly important for the crustal earthquake catalog because the sources of non-tectonic seismic events are typically shallow (for example blasts generated in mines, quarries, and roadcuts; volcanoes; atmospheric phenomena). In the crustal earthquake catalog non-tectonic events were identified by cross-checking the records with a list of mining-related events from the Pacific Northwest Seismic Network (PNSN) catalog. Earthquake activity associated with Mount St. Helens eruption was also excluded from the catalog. For historical records, the information collected by Ludwin (2006) was used to identify earthquakes of volcanic origin.

For the purpose of tracking all available information about the seismicity of the region, all records of non-tectonic events are maintained in the earthquake catalog database (see Appendix C, Section C.3.1), but they are not included in the final catalog and are not used in recurrence calculations. A flag and/or a comment, as appropriate, is placed on each non-tectonic or duplicate record in the catalog database to document the reason for its exclusion.

In the subduction catalog the main task is to separate crustal earthquakes (which may also include some non-tectonic events) from earthquakes associated with the Cascadia subduction zone. It should be noted that no separation is made between intra-slab and interface earthquakes because there are not enough focal mechanisms to allow a correct identification of the earthquakes. Earthquakes associated with the subduction zone are identified by comparing their focal depths with the depths of the top of the Juan de Fuca slab at the same location. The latter is obtained by interpolating the contour lines published by McCrory et al. (2006) at each epicentral location. Then, one of the following three criteria is applied:

1. If the earthquake's focal depth is greater than or equal to the top of the slab, the earthquake is assigned to the subduction catalog.
2. If the top of the slab is within the vertical solution error (when available) of the earthquake's epicentral location, the earthquake is assigned to the subduction catalog.
3. If a vertical solution error is unavailable but the difference between the earthquake's focal depth and the depth of the top of the slab is less than 20% of the depth of top the slab, the earthquake is assigned to the subduction catalog. This criterion is based on a trial-and-error procedure tested by plotting

depth cross sections of the subduction earthquakes with color-coded depths and then visually verifying that all earthquakes fall within the correct depth range. This criterion accounts for an uncertainty in the focal depth (even if it is not explicitly indicated) as well as an uncertainty in the location of the top of the slab.

The three criteria are schematically illustrated in Figure 6.1. Earthquake A has a well-constrained depth and is located below the top of the Juan de Fuca slab, so it will be assigned to the subduction catalog; this corresponds to the first of the criteria listed above. Earthquake B has a well-constrained depth and is located just above the top of the slab; however, accounting for the error on the solution there is a possibility that the earthquake might be below the slab. This earthquake is added to the subduction catalog according to the second criterion listed above. Earthquake C does not have a solution error but the difference between its focal depth and the depth of the top of the slab at the epicentral location is within 20%; therefore, according to the third criterion this earthquake is added to the subduction catalog. The last case is Earthquake D, which is a crustal earthquake because it is located at a shallower depth than the top of the Juan de Fuca slab.

As noted in Chapter 7.0, the approach described above for identifying subduction zone earthquakes for purposes of the SSC model is different from the algorithm for earthquake classification used by the GMC model. The Garcia et al. (2012) algorithm was selected for GMC applications because it is specifically targeted at ground motion prediction equation selection. Because the objectives of earthquake classification for the SSC catalog and the GMC ground motion catalog are different, there are no implications of using different algorithms on the computed hazard.

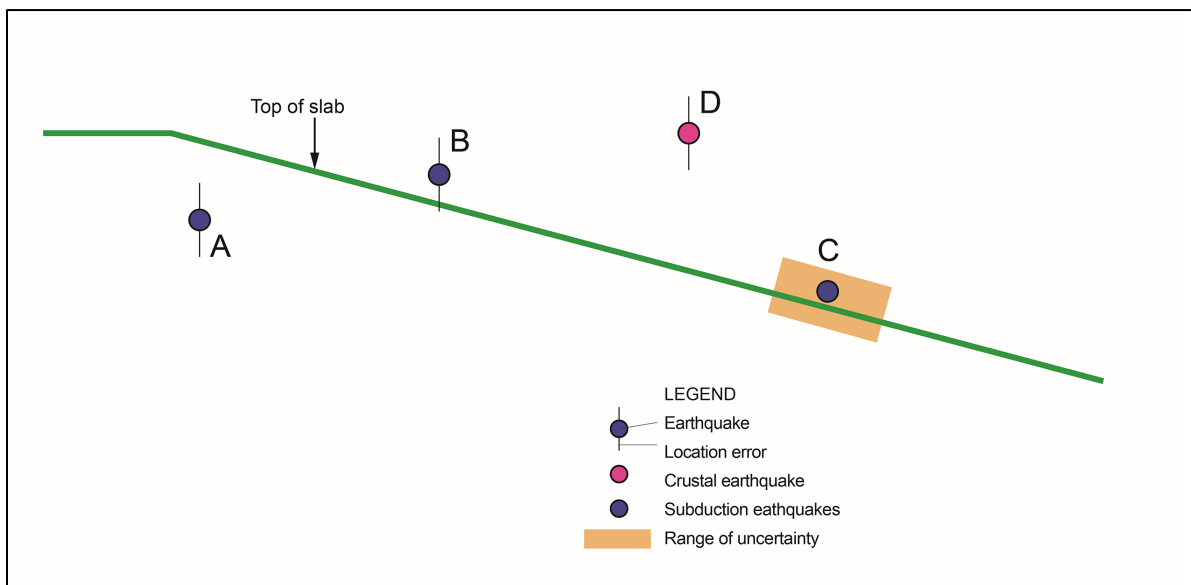


Figure 6.1. Schematic explaining the criteria for assigning earthquakes to the slab.

Several hundred earthquakes in the subduction catalog have either a fixed depth (i.e., a depth assigned by the location algorithm or by a geophysicist) or no depth. Typically these listings are older instrumental records (pre-1969) or historical earthquakes. In the absence of specific information about these earthquakes, it is impossible to establish their nature. For this reason, two separate subduction catalogs are created for the purpose of computing recurrence rates: in one catalog all the earthquakes with unknown or fixed depth are excluded; in the other catalog they are all included.

6.1.4 Time Span Covered

The crustal earthquake catalog covers the time period from the earliest reported earthquake (dated November 24, 1866) to midnight on April 30, 2013. All times are entered as Greenwich Mean Time (GMT); historical earthquakes reported with local (Pacific) time have been converted to GMT by adding 8 hours. Daylight savings time is not considered because it was not enforced at the time of these earthquakes.

The earliest earthquake reported in the subduction earthquake catalog occurred on February 17, 1793, but does not have an associated depth. As discussed above in Section 6.1.3, if the earthquakes with no depth or fixed depth are removed from the catalog the earliest earthquake in the subduction catalog occurred on January 11, 1909. In both cases, the subduction catalog spans from the earliest available record to midnight April 30, 2013.

6.2 Earthquake Record Sources

The compilation of the earthquake catalogs for this project followed three main steps. First, all of the available records from national and local catalogs were obtained for earthquakes that occurred within the areas listed in Section 6.1.1. Each record was assigned an alphanumeric record identification number composed of a catalog identification code followed by a sequential number. Then the records were sorted by date and time and carefully reviewed to identify duplicates. Lastly, for each earthquake one record was selected among the duplicates to represent the best solution (see Section 6.2.5 for details). This record was assigned a unique, sequential earthquake identification number without a catalog code. All of the available magnitude estimates were preserved in the selected earthquake record.

The sources of earthquake records can be grouped in the following categories: sources of data on historical (pre-instrumental) seismicity, continental-scale catalogs, regional-scale catalogs, previous composite earthquake catalogs, and studies of individual earthquakes. Figure 6.2 shows the regional distribution of catalogs used to compile the crustal and subduction catalogs used for this project.

6.2.1 Historical Seismicity

The composite earthquake catalog consists of historical records and instrumental records. The first instrumental recordings in this region appear in the 1930s; however, it is not until 1969 when the PNSN began operation that earthquakes were systematically recorded in the regions of interest for this project.

The Historical Earthquake Catalog of Eastern Washington (Rohay 1989) contains 105 earthquakes that occurred in the region of the crustal earthquake catalog between 1866 and 1979. The document lists macroseismic intensities ranging between IV and VII on the modified Mercalli intensity (MMI) scale, and for some events (starting in 1925) there is also an instrumental magnitude (typically local magnitude (M_L)), but the catalog also includes some body-wave magnitude (m_b) and the coda-wave magnitude (M_C).

Additional sources of information about pre-instrumental seismicity are the Cascadia Historical Earthquake Catalog compiled and maintained by PNSN and the Stover and Coffman (1993) report about significant earthquakes that have occurred in the United States. The Cascadia Historical Earthquake Catalog spans from 1793 to 1929 and is a compilation of accounts from earlier earthquake catalogs and

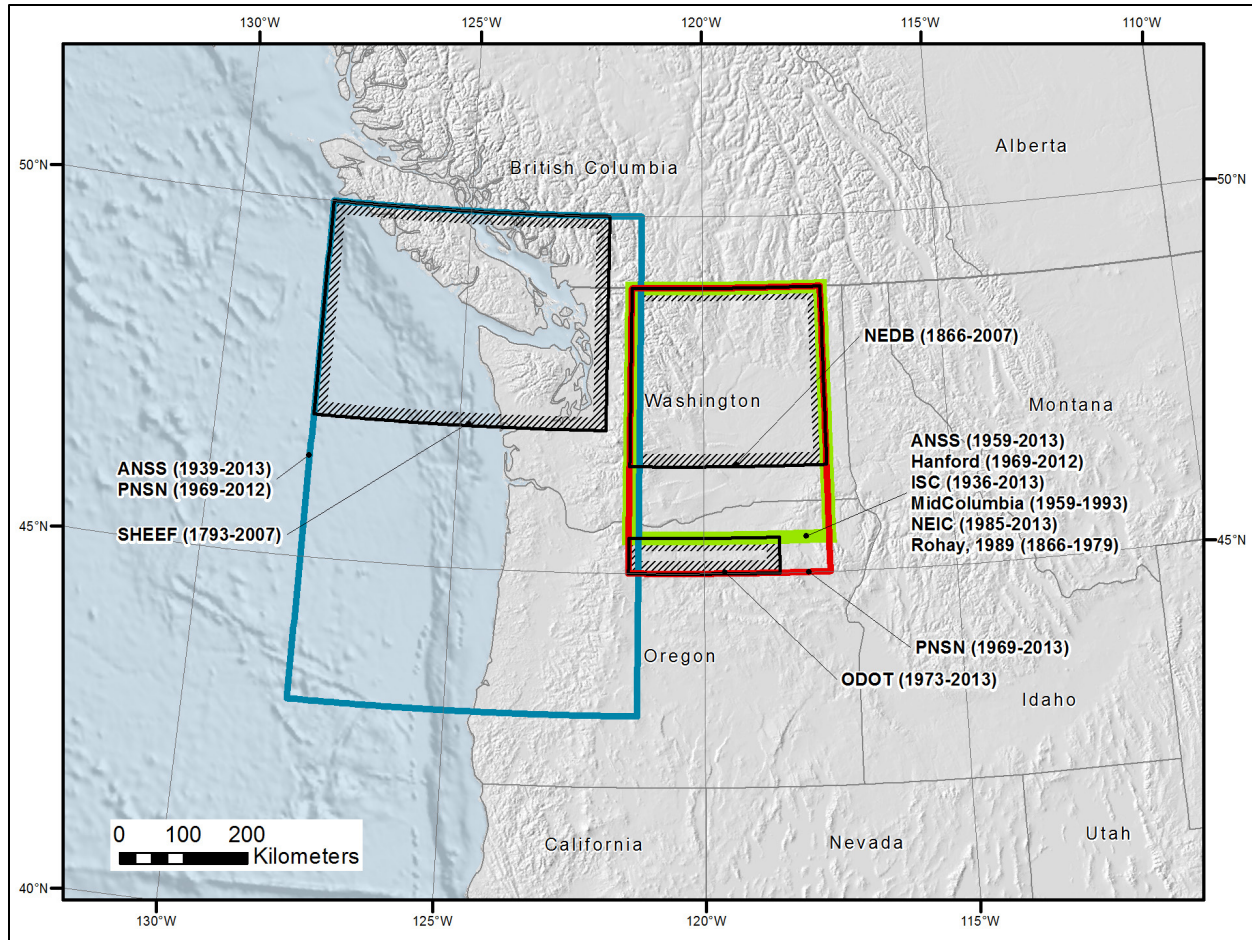


Figure 6.2. Map of the regional distribution of catalogs used to compile the crustal and subduction catalogs.

other sources, including newspaper articles, weather observers' reports, and diary entries. Stover and Coffman's (1993) report is a collection of significant earthquakes that occurred in the United States from 1568 to 1989. A review of the information contained in this publication for the states of Washington and Oregon provided several values of epicentral intensity and felt area. These data were added to the corresponding earthquake record of each earthquake in the catalog.

Most of the information for pre-instrumental earthquakes in Cascadia, possibly associated with the subduction zone, is obtained from the Geological Survey of Canada (GSC) Seismic Hazard Earthquake Epicenter File (SHEEF; Halchuck 2009), which was used for the compilation of the National Seismic Hazard Maps of Canada.

6.2.2 Regional-Scale Catalogs

The primary sources for the compilation of the crustal earthquake catalog were the Hanford Catalog and the PNSN catalog. The latter is the primary source of data for the subduction earthquake catalog for the time period between 1969 and 2012.

The Hanford seismic network routinely reports earthquakes occurring in the region of interest.¹ The catalog includes 11,753 earthquakes recorded from 1969 to January 18, 2012, each with an estimate of duration magnitude (M_D). Seventeen records were excluded from the Hanford crustal catalog because they were located outside of the region boundaries specified in Section 6.1.1.

A custom search on the PNSN website returned 15,241 earthquake records within the crustal catalog area (see Figure 6.5 in Section 6.3.1). The PNSN catalog provides an estimate of M_D except for recent (post-2006), large and well-recorded earthquakes for which M_L is calculated instead (Alan Rohay written communication to Valentina Montaldo-Falero, May 7, 2013).

6.2.3 Continental-Scale Catalogs

In compiling the crustal earthquake catalog, continental-scale catalogs were used mostly to obtain additional information about the size measure of earthquakes. The continental-scale catalogs, in fact, typically rely upon information from local networks such as the Hanford seismic network or PNSN. In the case of the subduction earthquake catalog, however, the lack of information from local networks in the pre-instrumental period makes it more compelling to find information from national and Canadian catalogs. The main continental-scale catalogs used in this project are briefly described below.

- The Advanced National Seismic System (ANSS) catalog lists 6,775 records of earthquakes between 1959 and April 30, 2013 in the crustal earthquake catalog region and more than 10,000 in the subduction catalog region. The majority of the records come from the PNSN, but ANSS magnitudes are listed as M_C , even though the PNSN calculates M_D . Also, the ANSS reports seconds and depths with more significant digits than the corresponding records obtained directly from the PNSN.
- The National Earthquake Information Center (NEIC) catalog lists 381 earthquakes in the crustal catalog region, most of which (288) have M_D ; the remaining records have M_L , m_b , or moment magnitude (M_w).
- The GSC maintains a database of earthquakes (the National Earthquake Data Base [NEDB]) recorded by various Canadian regional networks; it was used to retrieve 267 earthquake records in the crustal catalog region. The data are typically located north of 48° north, with only a couple of events as far south as the Yakima folds. As described previously, the SHEEF is the primary source of pre-instrumental records in the subduction catalog. Records prior to 1930 were augmented with macroseismic information from the Cascadia Historical Earthquake Catalog described in Section 6.2.1.
- The mission of the International Seismological Centre (ISC) is to collect and analyze seismic data from around the world and produce a bulletin that summarizes the information. The ISC catalog was used mostly to add information about the size measure of various earthquakes. The magnitudes listed in the ISC catalog are obtained from a number of different sources, including PNSN, USGS, GSC, USArray, Montana Bureau of Mines and Geology, but also foreign agencies (e.g., NORSAR), which use teleseismic data to determine magnitudes. Teleseismic data are listed in the catalog but were not used to calculate the uniform magnitude.

¹ The Hanford earthquake catalog was transmitted by Alan Rohay to Valentina Montaldo-Falero via email on May 8, 2013.

- In the recent past, the USGS has begun collecting information about the felt intensity of earthquakes through a dedicated website called “Did you feel it?” Citizens who feel an earthquake can complete a questionnaire online, and the data collected are then processed to obtain MMIs. Data from Washington, Oregon, Idaho, and British Columbia were retrieved and used to add the maximum observed intensity to the corresponding earthquake records in the catalog.

6.2.4 Previous Catalog Compilation Efforts

The earthquake catalog used for the Mid-Columbia Dams project (JBA et al. 2012) covers the area between latitude 40.5°N and 66.5°N, and longitude -110°E to -141°E. The catalog is largely based on pre-existing catalogs prepared for use in various regional seismic hazard assessments in the Pacific Northwest. For the Mid-Columbia project catalog, historical events (pre-1969) were primarily obtained from Ruth Ludwin at the PNSN (catalog from 1841 to 1934), Hanford, and USGS compilations; instrumental records were obtained from the ANSS (called CNSS at the time of that study), data from the University of Washington, and the USGS. The catalog spans from 1841 to May 2007.

The Geomatrix (1995) earthquake catalog was compiled for a PSHA study conducted for the Oregon Department of Transportation. The catalog covers the area extending from latitude 40°N to 50°N, and from longitude -115°E to -128°E and is a compilation of five catalogs (Decade of North American Geology; Northern California Seismic Network; University of Washington Network; University of Nevada, Reno, Network; and Boise State University Network) covering different areas and time periods. The catalog covers the time period between November 27, 1827 and November 30, 1993.

6.2.5 Identification of Unique Earthquake Entries

The process of merging multiple earthquake catalogs causes some duplication of records for the same earthquakes. The last step of the catalog compilation process is to select one record among the duplicates to represent each earthquake. For smaller earthquakes there are typically only two or three records from which to select (Hanford network, PNSN, ANSS), but for large, recent earthquakes there may be more. The selection of the preferred record in the crustal earthquake catalog is based on an order of preference that attributes first priority to records from the Hanford network, or the PNSN, based on the generally good quality of their solutions. If neither is available, the ANSS is preferred, and finally Mid-Columbia or Oregon Department of Transportation records (mostly in the pre-instrumental part of the catalog). In compiling the subduction catalog, preference was given to records from the Seismic Hazard Earthquake Epicenters File (SHEEF; Halchuk, 2009) in the pre-1969 time window, then the PNSN between 1969 and 2012, and the ANSS (listing PNSN solutions) after that.

The selection was done manually by carefully reviewing the catalog and cross-checking information reported in the various catalogs. The process of reviewing the records also enabled the time, and sometimes the date, of historical records that had been entered in local time instead of GMT to be corrected. For example, the Mid-Columbia catalog reports an earthquake on April 6, 1875, at 4:15 PM and lists an earlier catalog by Ludwin as the source. A cross-check with the Cascadia Historical Earthquake Catalog shows that the time (4:15 PM) is Pacific time. The selected record for this earthquake corresponds to the Mid-Columbia location, but with the date and time corrected to GMT, April 7, 1875, at 00:15 AM. For other historical records, macroseismic intensities originally determined using the Rossi-Forrel scale were incorrectly reported as MMI; according to the comparison chart by Richter (1958) the two scales are identical for low-intensity levels (I, II, and III), but for larger intensities they differ by about half of an intensity level.

As discussed earlier in this section, the record selected to represent the earthquake is assigned a unique identification number and all available magnitudes are copied from the duplicate entries to the preferred record. It should also be noted that any modification to the date, time, or intensity is made to the preferred record and is documented with a comment in the earthquake catalog database (see Appendix C, Section C.3.1).

6.3 Epicentral Locations

Figure 6.3 shows the distribution of seismicity in the area covered by the crustal earthquake catalog. The seismicity is mostly concentrated in the YFB, where it is observed to contain numerous small-to-large shallow earthquake swarms, and in the aftershock area near Lake Chelan. In the easternmost part of the area earthquakes are more sparse. The locations of earthquakes associated with the Cascadia subduction zone are shown in Figure 6.4. The map shows that the highest density of earthquakes occurs in the Puget Sound area, and it decreases to the south and to the northwest.

Records of earthquakes that occurred before 1936 are considered pre-instrumental. These are typically obtained from written accounts of observers, who describe the effect of the earthquake at a given location. A measure of the earthquake intensity is obtained from the various accounts and the epicentral location is inferred from the distribution of the maximum damage. The accuracy of these estimates is largely dependent on the number and accuracy of the original accounts. In addition, the detection threshold in the pre-instrumental period is rather large, because only earthquakes that were severe enough to be worth writing about were being reported.

During the early instrumental period, between 1936 and the installation of the PNSN in 1969, the number of seismographs increased progressively and with it the accuracy of earthquake locations; at the same time, the detection threshold became lower. According to Ludwin et al. (1991), the detection threshold of the PNSN was about 4.5 until 1970.

Figure 6.5 shows a map of the crustal earthquakes where pre-instrumental earthquakes are represented by yellow triangles and early instrumental earthquakes by green squares. Instrumental seismicity is superimposed and represented by pink circles. The figure shows that there are more early instrumental and instrumental earthquakes than pre-instrumental records, which is consistent with lower magnitude detection thresholds as time progresses. The locations of the pre-instrumental and early instrumental earthquakes are generally in good agreement with the recent seismicity, but there is a significant lack of pre-1969 earthquakes in the central part of the YFB.

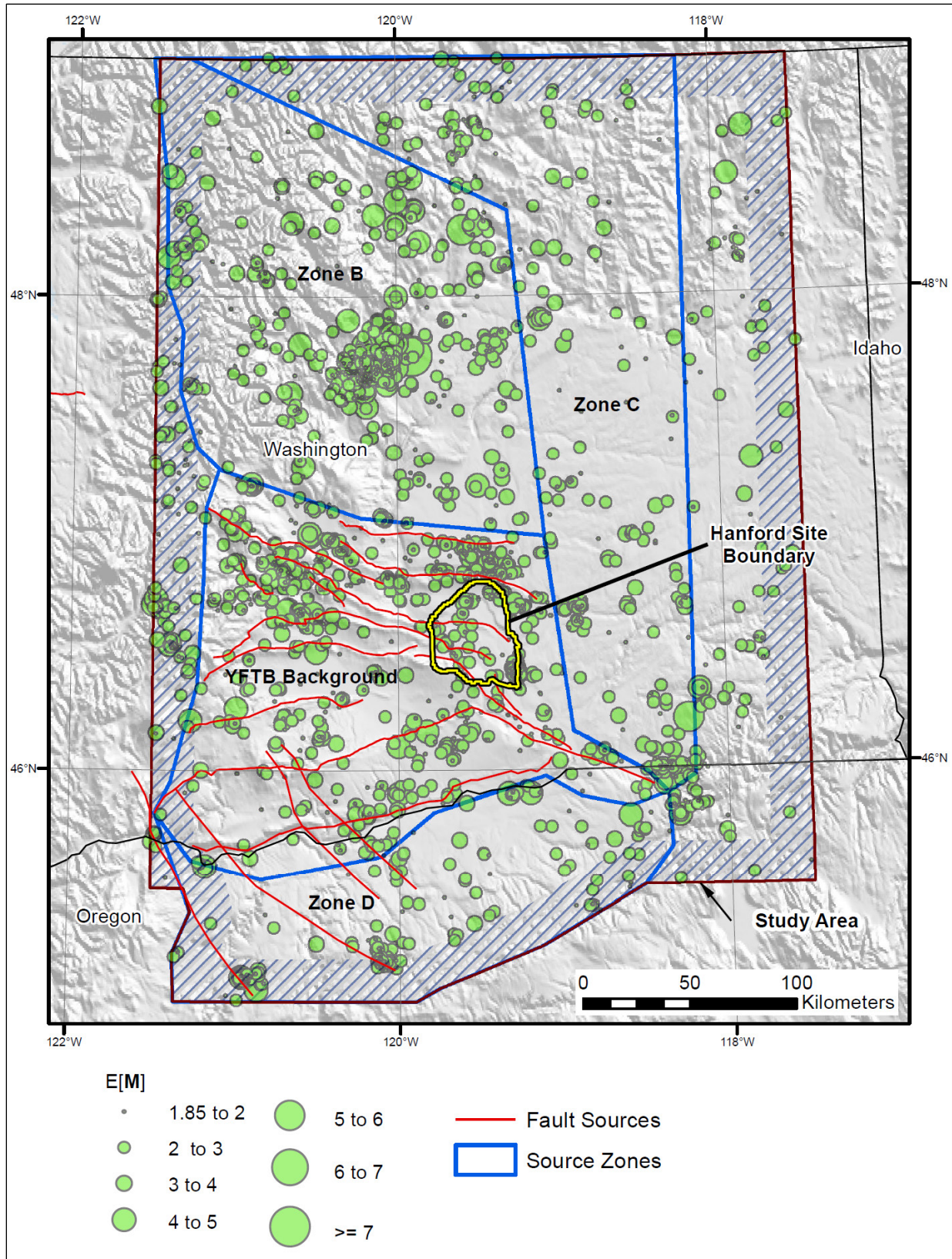


Figure 6.3. Distribution of seismicity in the area covered by the crustal earthquake catalog. Magnitude values used in the plots are E[M] values (see Section 6.5.2).

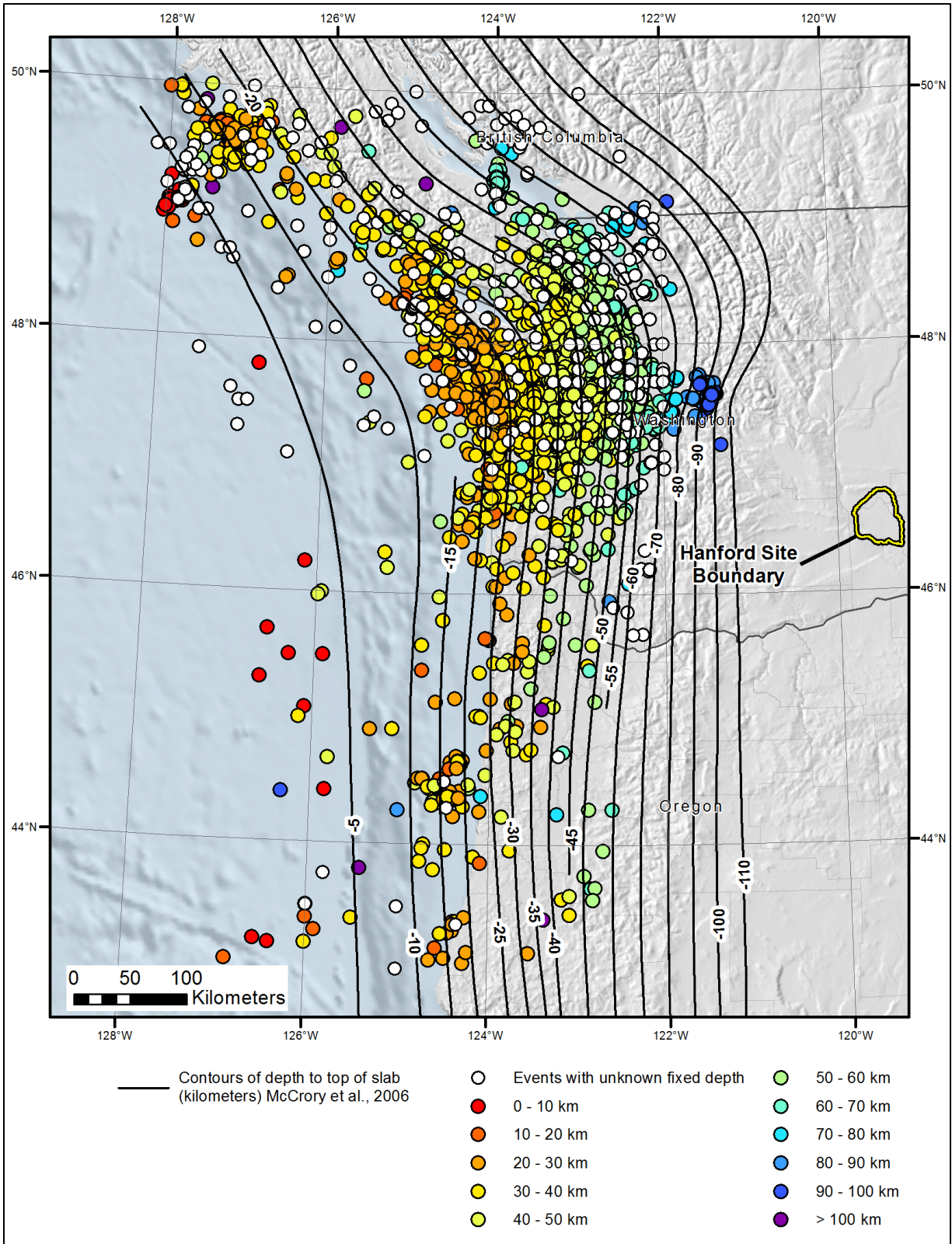


Figure 6.4. Distribution of seismicity in the area covered by the subduction earthquake catalog.

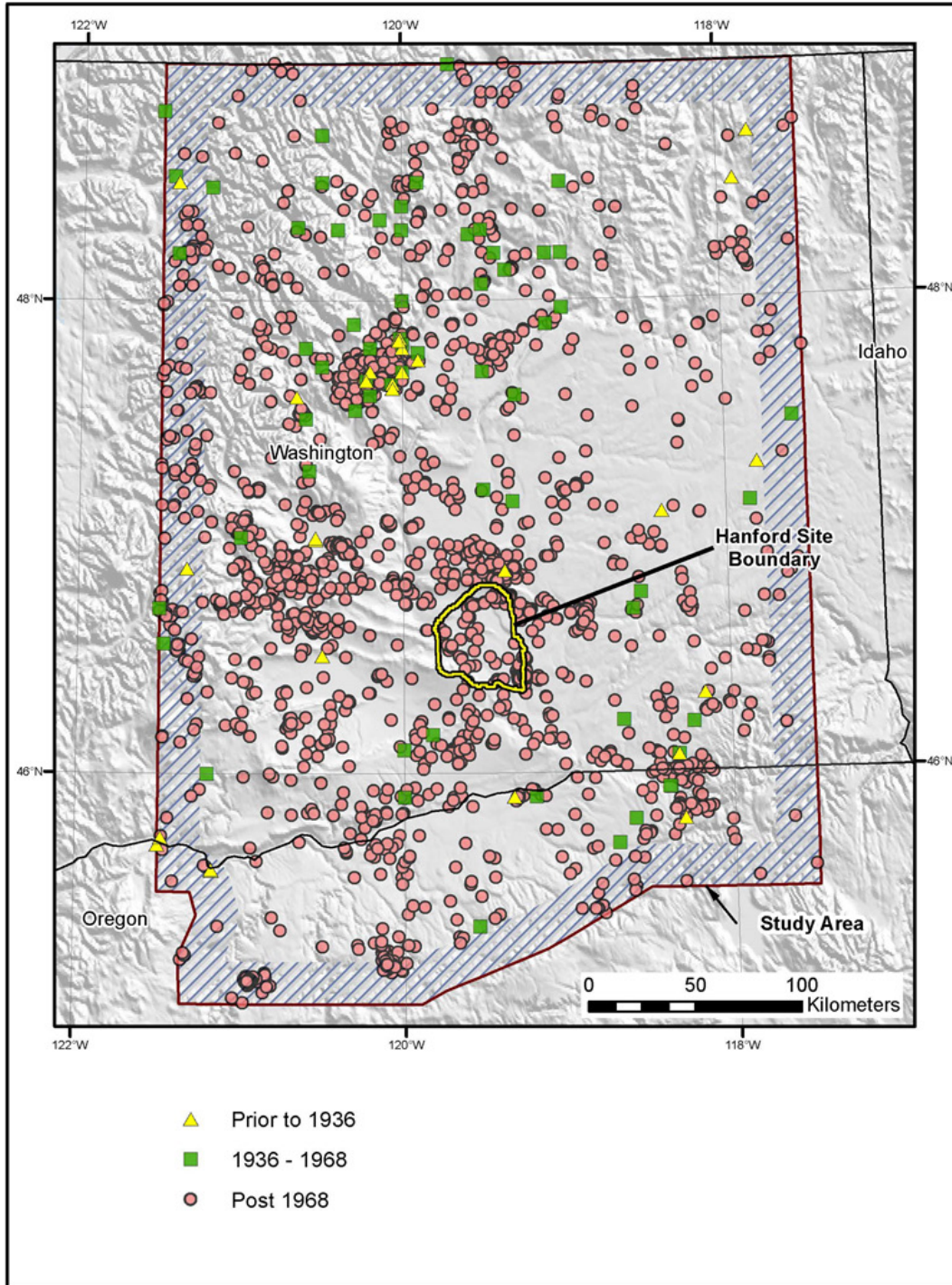


Figure 6.5. Map of earthquake epicenters in the crustal catalog recorded during the pre-, early, and modern instrumental periods. Magnitude values used in the plots are E[M] values ranging from 1.85 to 7.06 (see Appendix C).

6.4 Focal Depth

Modern instrumental earthquake catalogs contain an estimate of the focal depth of the earthquakes. As discussed earlier, focal depth is a key parameter in assigning earthquakes to the subduction catalog; focal depth is also important for the assessment of the seismogenic crustal thickness.

6.4.1 Routine Location Procedure and Depth Determination

High-resolution seismicity analyses show that the resolution of the PNSN routine epicentral location is good; horizontal and vertical errors are generally smaller than 2 km (see Appendix F).

6.4.2 Spatial Variation of Depth Distribution Across Study Region

Focal depths are available for approximately 10,000 instrumentally recorded crustal earthquakes excluding fixed depths. In most catalogs fixed depths are identified by a letter or a character that indicates whether the depth was constrained to allow the solution for other unknown parameters to converge, or if the maximum number of iterations was exceeded without meeting convergence tests, and both location and depth have been fixed. Typical values assigned to fixed depths are 10, 18 (for Canadian data), or 33 km for crustal earthquakes.

Four cross sections have been prepared to show the distribution of crustal earthquakes at depth: two of these cross sections are east-west trending at latitudes 46.5°N (Figure 6.6e) and 47.5°N (Figure 6.6d); the other two cross sections are north-south trending at longitudes -119.5°E (Figure 6.6c) and -120.5°E (Figure 6.6b). The seismicity shown in the cross sections is collected within a 0.1-degree band. Figure 6.6e shows that in the central part of the area, corresponding to the Yakima folds, the seismicity is distributed within the first 25 km. To the east of this central region, focal depths are limited to within the first 5 km. Figure 6.6d shows that most of the seismicity to the north of the Yakima folds occurs within the first 10 to 15 km. The westernmost cross section (Figure 6.6b) shows deeper earthquakes (20 to 30 km deep) to the south and shallower earthquakes to the north. In the eastern cross section (Figure 6.6c) the seismicity seems to be distributed more uniformly through the first 20 km. The cross section shows a gap of seismicity between 5 and 10 km just north of the Yakima folds, but this is likely because there are no earthquakes in this location.

Figure 6.4 shows the subduction earthquakes color-coded by focal depth in comparison with the depth contours of the top of the Juan de Fuca slab by McCrory et al. (2006). Focal depths range from approximately 0 to 10 km offshore to more than 100 km to the east. Figure 6.7 is a cross section roughly perpendicular to the contour lines that collects seismicity from the Olympic Peninsula and Puget Sound to the west and connects to Figure 6.6a to the east. The seismicity offers a good representation of the slab and indicates a steepening of the slab east of -122.5°E.

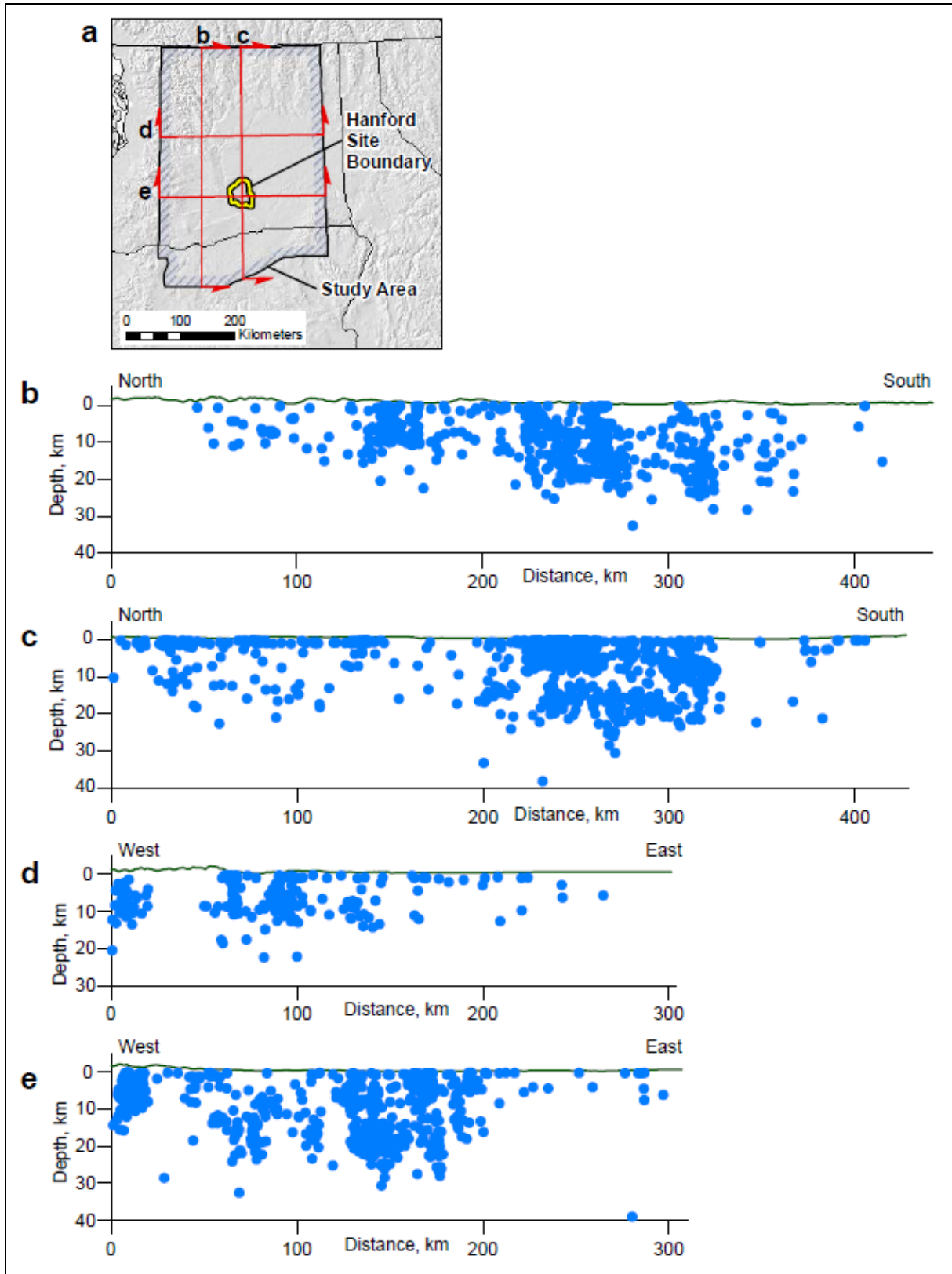


Figure 6.6. (a) Map showing the cross-section location, (b) cross section at -120.5°E , (c) cross section at -119.5°E , (d) cross section at 47.5°N , and (e) cross section at 46.5°N .

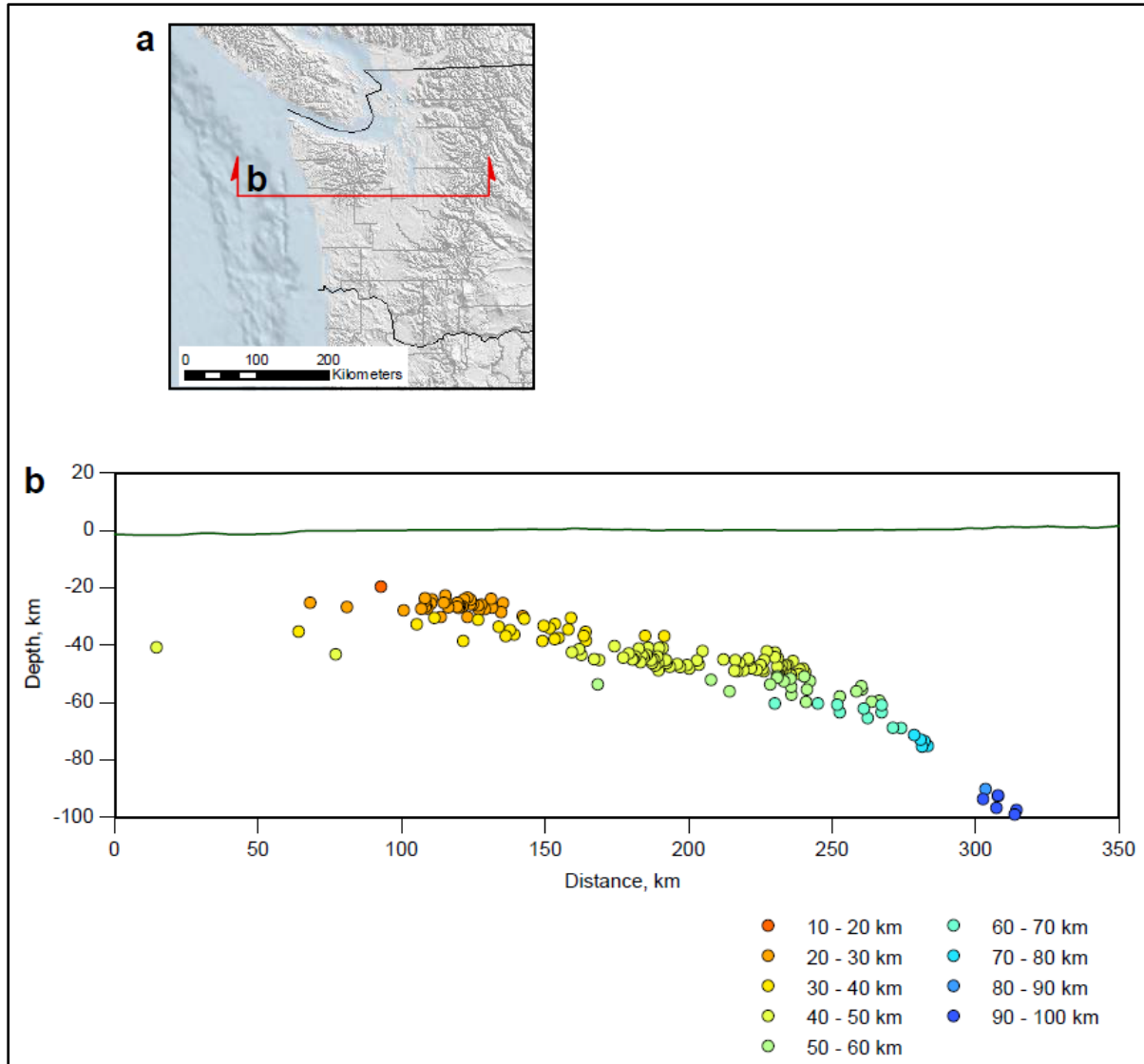


Figure 6.7. Cross section drawn along the transect shown in panel (a). Panel (b) shows hypocenters along the transect from subduction catalog. Hypocenter depths are color-coded.

6.5 Magnitude Homogenization

The earthquake catalog is used in PSHA to obtain earthquake recurrence parameters for source zones, and it is important that a uniform earthquake size measure be used in the catalog. In modern PSHA studies this measure is chosen to be consistent with the magnitude scale used in the applicable ground motion predictive relationships. The ground motion models used in the Hanford PSHA are defined in terms of moment magnitude, so the catalogs of crustal and subduction earthquakes need to be uniformly converted to moment magnitude. The approach presented in NUREG-2115 (NRC 2012) to obtain uniform magnitudes and the use of N^* to obtain unbiased recurrence calculations are used in this project.

6.5.1 Target Magnitude and Available Magnitudes

Based on the discussion above, for the earthquake catalogs to be consistent with the size measure used in the ground motion predictive models, they need to be converted to a uniform estimate of M_W . However, M_W is available only for a small number of earthquakes in the Hanford catalogs. Most of the earthquake records report M_D because they are obtained from the Hanford and PNSN catalogs, or M_C because they are obtained from the ANSS. Together M_D and M_C represent 95% of the magnitude values in the crustal earthquake catalog compiled for this project. The remaining magnitude values are divided between M_L , m_b , surface-wave magnitude (M_S), and macroseismic intensity (I_0). Similarly, in the subduction catalog most of the earthquake records have M_D or M_C , and M_L , M_S , or m_b . Table 6.1 and Table 6.2 show the magnitude types and the ranges of values observed in the crustal and subduction catalogs. In general, this study uses M_W to indicate moment magnitudes determined by various agencies and reported in their catalogs, whereas \mathbf{M} is used for moment magnitudes calculated from seismic moment using Hanks and Kanamori (1979). Exceptions are the four earthquakes listed in Table 6.1 with magnitudes \mathbf{M} : these magnitudes are reported as \mathbf{M} in the ISC catalog that lists various agencies (e.g., NEIS, now NEIC, Large Aperture Array) as the originators.

Table 6.1. Magnitude types and magnitude ranges in the crustal earthquake catalog.

Magnitude Type	No. Earthquakes	No. Mag. Values	Time Period	Magnitude Range
mb	25	42	1963 to 2011	2.9 to 5.0
Ms	15	20	1918 to 2011	2.0 to 5.8
ML	492	514	1936 to 2013	0 to 6.1
Mc	6719	7565	1969 to 2011	0.02 to 5.0
MD	7155	7155	1959 to 2013	-1.6 to 4.7
Mw	5	6	1994 to 2011	3.27 to 4.02
\mathbf{M}	4	4	1974 to 1975	3.0 to 4.4
I_0	233	238	1866 to 2013	I to IX

Table 6.2. Magnitude types and magnitude ranges in the subduction earthquake catalog.

Magnitude Type	No. Earthquakes	No. Mag Values	Time Period	Magnitude Range
m_b	36	41	1949 to 2012	3.1 to 6.9
Ms	8	10	1949 to 2012	4.1 to 6.1
Mc	1723	1727	1969 to 2012	0.1 to 6.8
Md	100	100	1992 to 2013	0.54 to 2.66
ML	236	236	1961 to 2013	1.74 to 5.9
Mw	10	12	1994 to 2013	4 to 6.2
\mathbf{M} from M_0	11	11	1949 to 2012	4.91 to 6.82
I_0	5	5	1909 to 2001	IV to VIII MMI
lnFA (km^2)	3	3	1909 to 1928	11.2 to 11.9

To be able to derive conversion equations it is necessary to have a database of earthquakes with at least one M_W and one other magnitude type. For the purpose of this analysis, M_w and \mathbf{M} are assumed to be the same, although work conducted in the Central Eastern United States-SSC project has shown that agencies are not always consistent in the way moment magnitudes are estimated. Without knowing the seismic moment, however, it is not possible to assess \mathbf{M} . Because the data in the project catalogs are insufficient for this kind of determinations, the data sets used in the regression analysis were augmented with earthquake records from nearby regions, in particular data from western Washington, Oregon, Montana, and Idaho were obtained from the Catalog of Moment Tensors for Parts of North America

(Saint Louis University 2013; 61 earthquakes) and from the Harvard Centroid Moment Tensor (HCMT) catalog (13 earthquakes). After testing to confirm that the data do not show different trends, crustal and subduction earthquakes were combined in one data set; note that offshore earthquakes associated with the Blanco Ridge and the Explorer plate are excluded from the analysis, as is the M 5.3 earthquake associated with Mount St. Helen's explosion.

The moment magnitude was consistently calculated for all the earthquakes obtained from the HCMT catalog and the Catalog of Moment Tensors for Parts of North America using the published Hanks and Kanamori (1979) formula:

$$M = 2/3 \log_{10}(M_0) - 10.7 \quad (6.1)$$

In cases where multiple values of moment magnitude are available, they have been combined in a weighted average using the formulation presented in NUREG-2115, assuming all estimates have equal weight. It should be noted that in the Hanks and Kanamori (1979) formula the coefficient 10.7 is rounded from 10.73; this different precision determines a 0.03-unit difference between the moment magnitudes published in the Catalog of Moment Tensors for Parts of North America and the corresponding magnitudes used in the Hanford catalog.

The ISC Earthquake Database was used to collect all possible magnitude estimates for the set of earthquakes that have a moment magnitude. The ISC database lists various types of instrumental magnitudes calculated by different agencies, including the NEIC, NEDB, the PNSN, and numerous other local and foreign agencies.

6.5.2 Conversion from M_c , M_D , and Other Magnitude Scales

The following subsections offer details about the empirical magnitude conversion relations derived for the magnitude types represented in the Hanford crustal and subduction catalogs. The data sets used to obtain these relations are provided in Appendix C, Section C.3.

6.5.2.1 Estimation of $E[M]$ from Moment Magnitude

Following NUREG-2115, the expected value of the true moment magnitude ($E[M]$) can be obtained from the observed moment magnitude (\hat{M}) given its uncertainty $\sigma[M|\hat{M}]$ using the following equation:

$$E[M|\hat{M}] = \hat{M} - \beta \sigma^2[M|\hat{M}] \quad (6.2)$$

where β is $b \cdot \ln(10)$. Based on a preliminary analysis of the data in the Hanford catalogs, the b value is assumed to be 0.95 for crustal earthquakes and 0.65 for subduction earthquakes.

Earthquake catalogs do not typically report the uncertainty in their magnitude estimates, but NUREG-2115 shows that an approximate estimate of $\sigma[M]$ can be obtained from the HCMT catalog. The average $\sigma[M]$ for the data set used for this project is equal to 0.051; given this value and consistent with findings in NUREG-2115, it is then assumed that a $\sigma[M|\hat{M}]$ of 0.1 is appropriate for earthquakes post-1980, while a $\sigma[M|\hat{M}]$ of 0.2 is appropriate for earlier earthquakes.

6.5.2.2 Estimation of $E[\mathbf{M}]$ from Body-Wave Magnitudes

The first step in deriving a conversion relation for m_b to $E[\mathbf{M}]$ consists of testing whether the data showed any significant trends with respect to regionalization, type of magnitude, or source. Figure 6.8a shows data from western Washington, the Hanford catalog, and Oregon; most of the data are in terms of m_b calculated from short-period waves. Other types of m_b —listed as M_b , MB , m_b1 , m_bmx , and m_btmp —are too few to show any trend or offset with respect to m_b . Also, the data do not indicate any significant difference between the regions. The data were then grouped by source agency and plotted in Figure 6.8b. A large number of magnitude values contained in the ISC catalog are determined by agencies in Europe or China, including several values from the International Data Center (IDC) for the Control of the Test Ban Treaty Organization in Vienna, Austria. These magnitudes introduce a large scatter in the data set and are not used to derive the conversion relations (unless IDC is the only available m_b estimate, in which case the data are maintained). Two m_b values for the earthquake that occurred in Oregon on July 14, 2008, are removed because they appear to be inconsistent with other m_b values for the same earthquake obtained by NEIC, as well as with the rest of the data set.

Figure 6.9 shows the results of the regression analysis conducted on the data set compared with the Sipkin (2003) model (light blue curve), which is the bilinear curve used by the USGS for the 2008 and 2014 National Seismic Hazard Maps (Peterson et al. 2008; 2014 maps [USGS In Preparation; <http://earthquake.usgs.gov/hazards/>]). The bilinear model that best fits the data is shown by the blue curve and has a break in slope at m_b 5.1, like the Sipkin (2003) model. This break point was selected after testing 12 alternative break points, from m_b 4.5 to 5.9, and using the Akaike Information Criterion (AIC) and the second-order AIC (AICc) to select the best model. For a given set of data the AIC is used to measure the relative quality of a statistical model based on the trade-off between the goodness of fit of the model and its complexity. The second-order AIC uses a greater penalty for additional parameters.

Figure 6.9 shows that a linear model (red curve) is not significantly different from the $\mathbf{M} = m_b$ line. The AIC, AICc, and the Bayesian Information Criterion (BIC) are applied to select between the linear and bilinear model and indicate a strong preference for the bilinear model over the linear model. As a result, the preferred magnitude conversion relation is as follows:

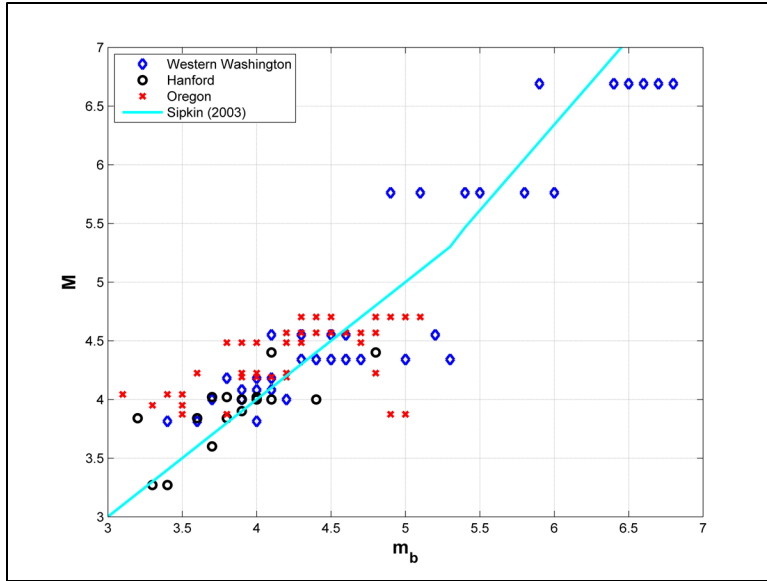
$$E[\mathbf{M}] = m \quad \text{for } m_b \leq 5.1 \quad (6.3)$$

$$E[\mathbf{M}] = -0.765 + 1.15 m_b \quad \text{for } m_b > 5.1$$

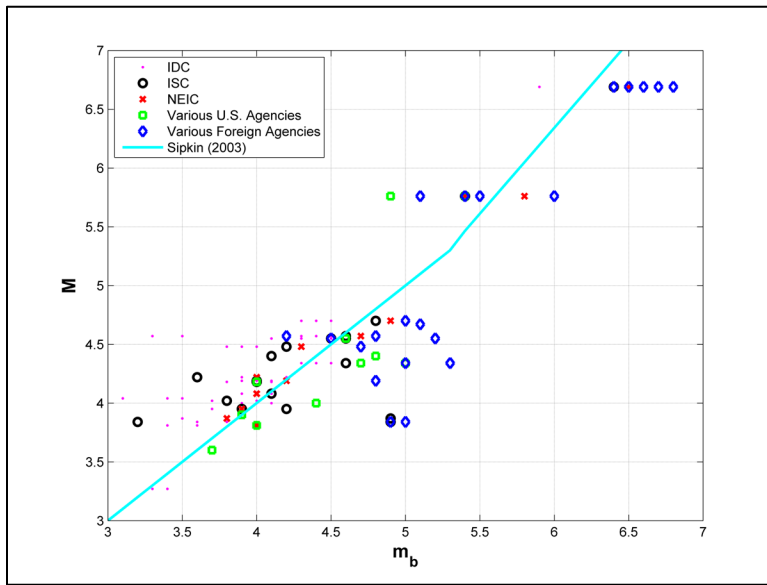
$$\sigma_{\mathbf{M}|m_b} = 0.24$$

Following NUREG-2115, $\sigma_{\mathbf{M}|m_b}$ is calculated as the difference between the sigma obtained from the regression (in this case 0.26) and the average value of $\sigma[\mathbf{M}|\hat{\mathbf{M}}] = 0.11$ for the earthquakes used in this regression.

Earthquakes with a m_b range in magnitude between 2.9 and 5 in the crustal catalog, and between 3.1 and 6.9 in the subduction catalog, and Equation 6.3 is applicable in the magnitude range of interest.



(a)



(b)

Figure 6.8. Relationship between m_b and M by (a) region and (b) source.

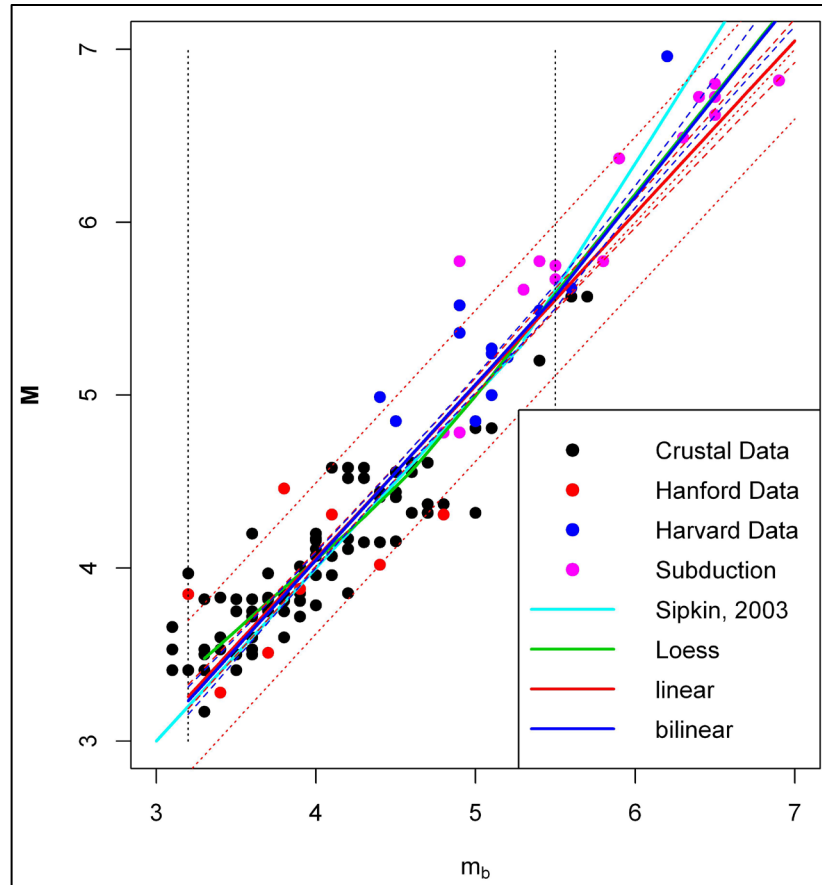


Figure 6.9. Regression of m_b and M .

6.5.2.3 Estimation of $E[M]$ from M_S Magnitudes

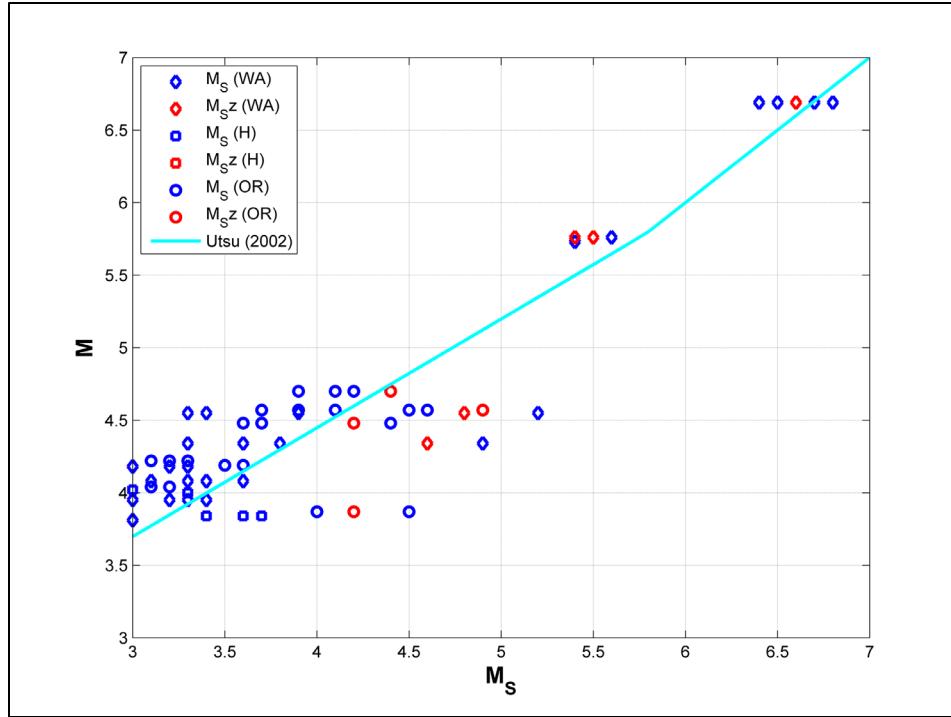
Surface-wave magnitudes (M_S) are computed from the amplitude of low-frequency surface waves; if the vertical component is used the magnitude is identified as M_{SZ} . Similar to the analysis described in the previous section, the plots in Figure 6.10 show that the data do not show any significant trend associated with regionalization or magnitude type, but that data from foreign agencies should be removed. Figure 6.11 compares the results of the regression analysis (shown by the blue curve) with the trilinear curve (light blue curve) used by the USGS in the 2008 and 2014 National Seismic Hazard Maps (Peterson et al. 2008; 2014 maps [USGS In Preparation; <http://earthquake.usgs.gov/hazards/>]), which is an approximation of the quadratic curve shown by Utsu (2002).

The fitted quadratic polynomial curve is given in Equation 6.4:

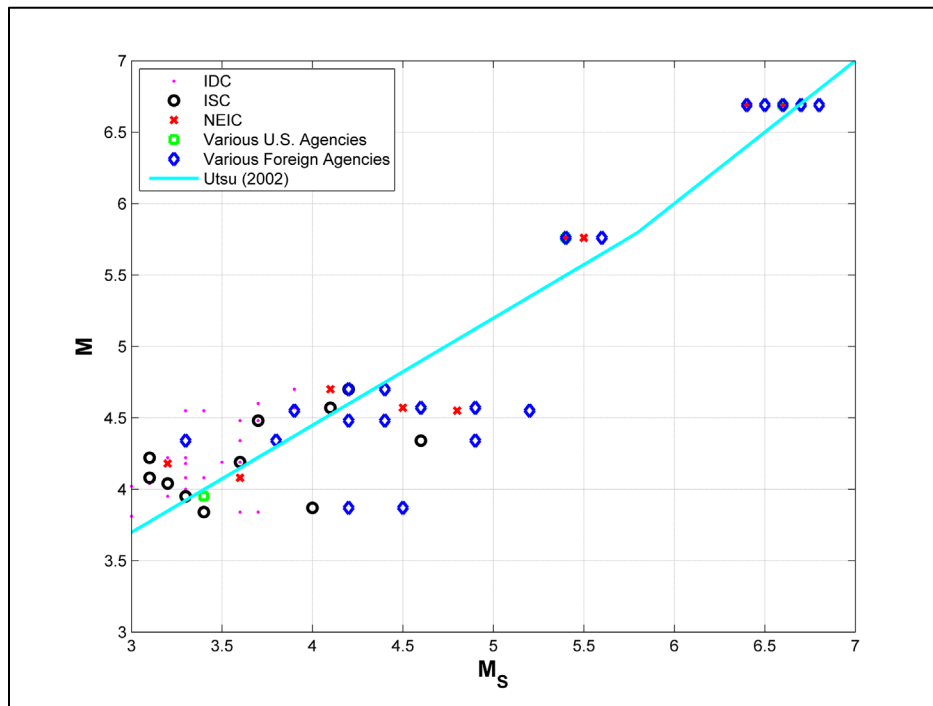
$$E[M] = 2.84 + 0.13 M_S + 0.07 M_S^2 \tag{6.4}$$

$$\sigma_{M|M_S} = 0.22$$

where $\sigma_{M|M_S}$ is calculated as the difference between the sigma of 0.24 obtained from the regression and the average value of $\sigma[M|\hat{M}] = 0.1$ for the earthquakes used in this regression.



(a)



(b)

Figure 6.10. Relationship between M_S and M by (a) region and M_S type, and by (b) source.

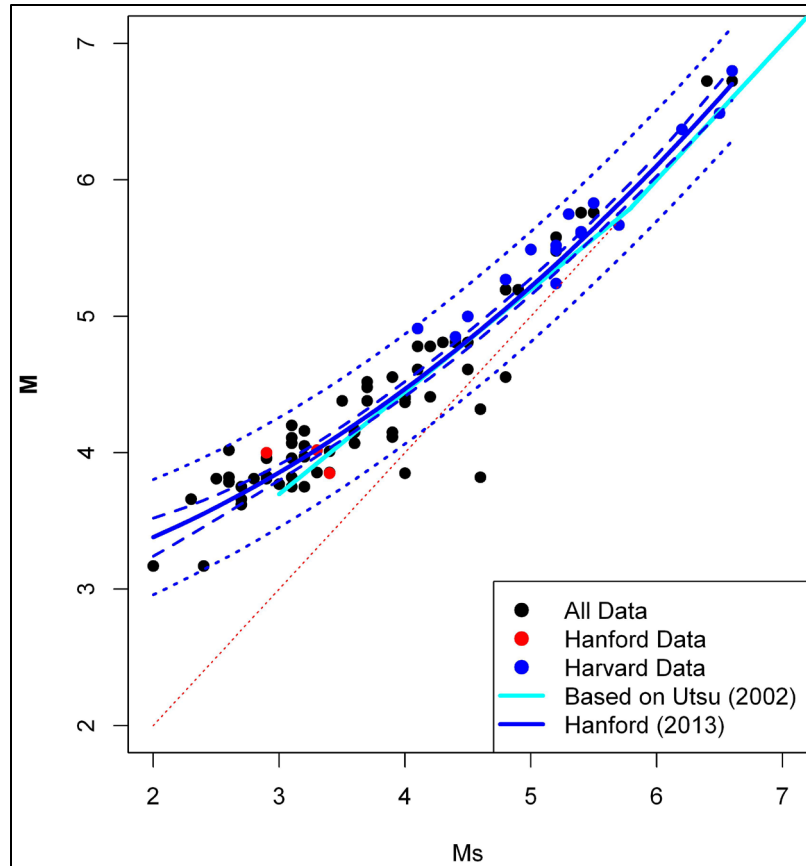


Figure 6.11. Regression of M_S and M .

Earthquakes with M_S range between 2.0 and 5.8 in the crustal catalog and between 4.1 and 6.6 in the subduction catalog, and the quadratic model is considered applicable in the magnitude range of interest.

6.5.2.4 Estimation of $E[M]$ from M_C and M_D Magnitudes

The majority of records in the Hanford crustal catalog have either M_C or M_D from the ANSS, PNSN, and Hanford network. To verify that M_C and M_D are in fact the same, earthquakes with M_D from the PNSN and M_C from other sources were selected from the crustal earthquake catalog. Figure 6.12 shows that the two magnitudes are generally consistent, except for a set of data points representing a decade of records (1970 to 1980) from the Mid-Columbia project catalog, therein referred to as “Hanford catalog from 1841 to 1980.” These earthquakes also have a record from the University of Washington with an associated M_C that is consistent with M_D . The M_C from the University of Washington has been retained, while the other M_C has been excluded from all subsequent analyses.

Approximately 1,300 records with M_C and M_D ranging from 0 to 4.6 have been compiled in the data set shown in Figure 6.12 for conducting regression analysis. The data are fitted by two models—a linear model (blue line) and an offset model (red line)—then the AIC and BIC tests are applied to select the best-fitting model. The results of these tests consistently favor the offset model, which has an intercept of 0.044. Based on this analysis it is assumed that M_C is equivalent to M_D . It should be noted that some of the differences between M_C and M_D shown in Figure 6.12 are likely caused by the different number of decimals with which the magnitudes are reported in the ANSS and PNSN.

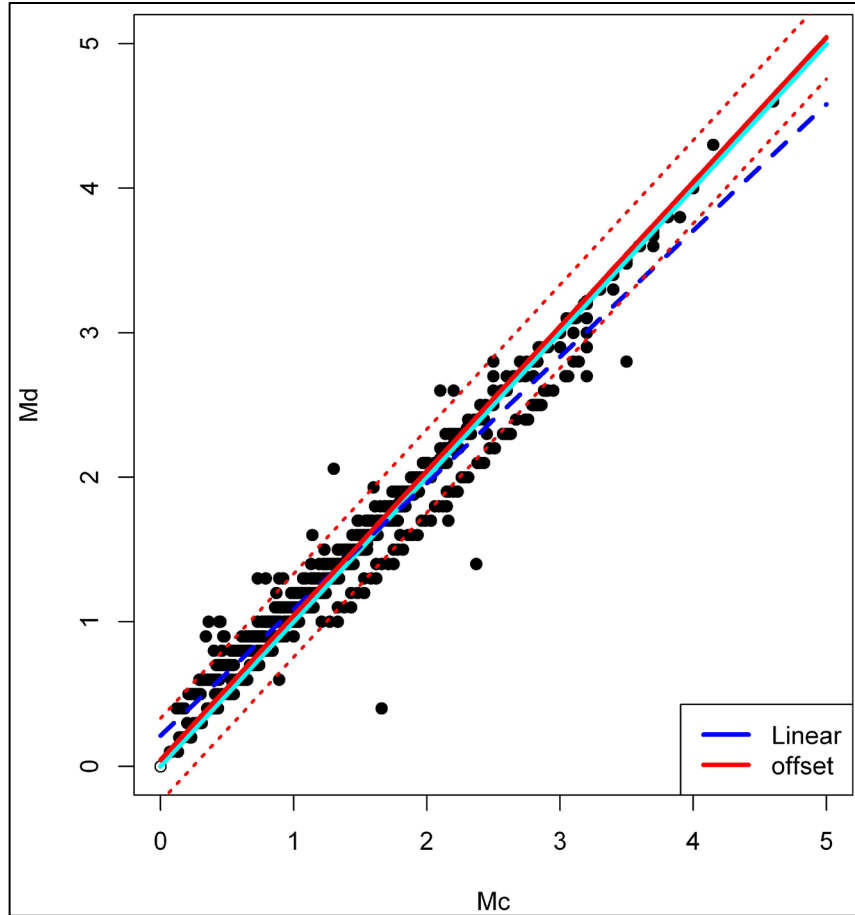


Figure 6.12. Relationship of M_C and M_D .

Because M_D and M_C are equivalent, both types of data are combined in a data set for use in the regression analysis. Figure 6.13 shows the results: both a linear curve (dashed blue line) and an offset model (red curve) have been fitted to the data. The two models are very similar, but the offset model produces consistently lower AIC and BIC results and it is preferred over the linear model. The resulting equation is as follows:

$$E[\mathbf{M}] = M_D - 0.15 \quad (6.5)$$

$$\sigma_{\mathbf{M}|M_D} = 0.19$$

Following NUREG-2115, $\sigma_{\mathbf{M}|M_D}$ is calculated as the difference between the sigma of 0.23 obtained from the regression and the average value of $\sigma[\mathbf{M}|\hat{\mathbf{M}}] = 0.13$ for the earthquakes used in this regression.

The crustal and subduction catalogs contain earthquakes with M_C in the range 0.1 to 6.8, and earthquakes with M_D in the range 0.54 to 2.7. Equation 6.5 is assumed to be applicable to both crustal and subduction earthquakes for $M_D \geq 2$.

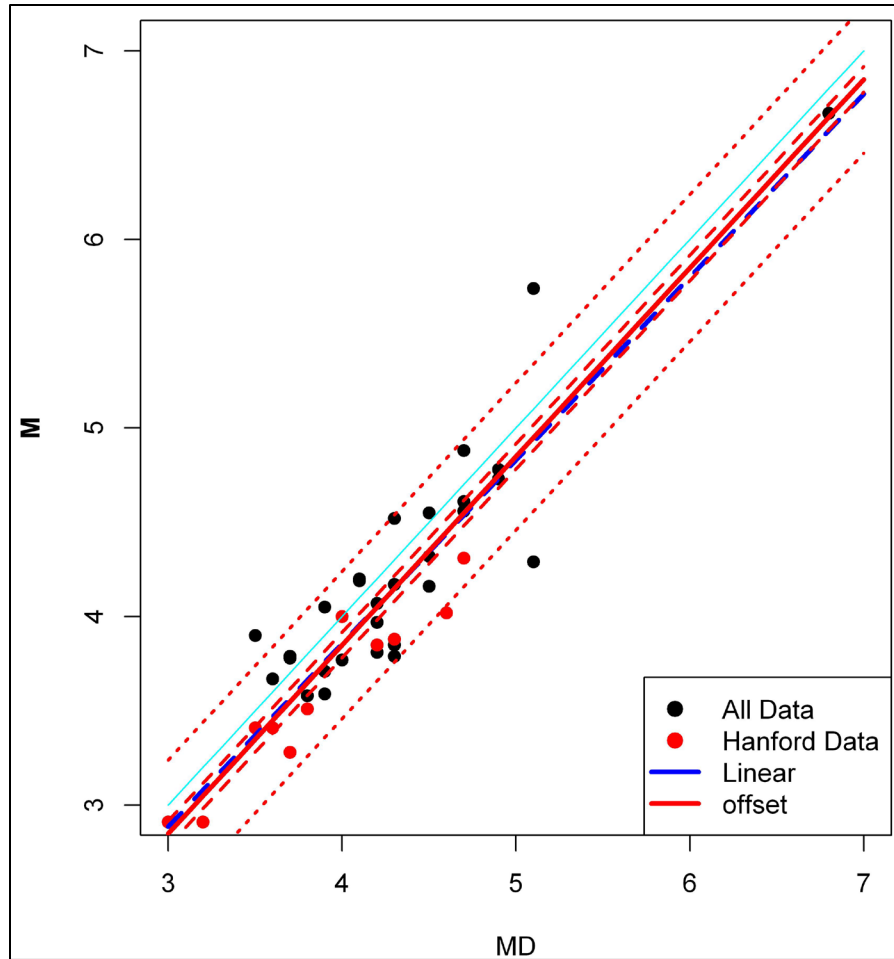


Figure 6.13. Regression of M_C and $M_D - M$.

6.5.2.5 Estimation of $E[M]$ from M_L Magnitudes

The Hanford crustal catalog contains approximately 500 estimates of M_L largely from small earthquakes (M_L ranging from 0.1 to 5), except for two estimates (M_L 5.75 and M_L 6.1) for the 1936 earthquake that are obtained from instrumental recordings. The subduction catalog contains more than 200 earthquakes with M_L ranging from 1.74 to 5.9. The data set available for regression analysis is limited to approximately M_L 4.5, as shown in Figure 6.14. Because the data are rather sparse, they were augmented by data with M and M_D , after converting M_D to M_L . First, all of the available records with M_D and M_L were fitted by both a linear and an offset model (see Figure 6.15). Use of different information criteria (AIC, AICc, and BIC) systematically indicates that the linear model should be favored over the offset model. The conversion from M_D to M_L is given in Equation 6.6.

$$M_L = 0.36 + 0.81 M_D \quad (6.6)$$

$$\sigma_{M_L | M_D} = 0.33$$

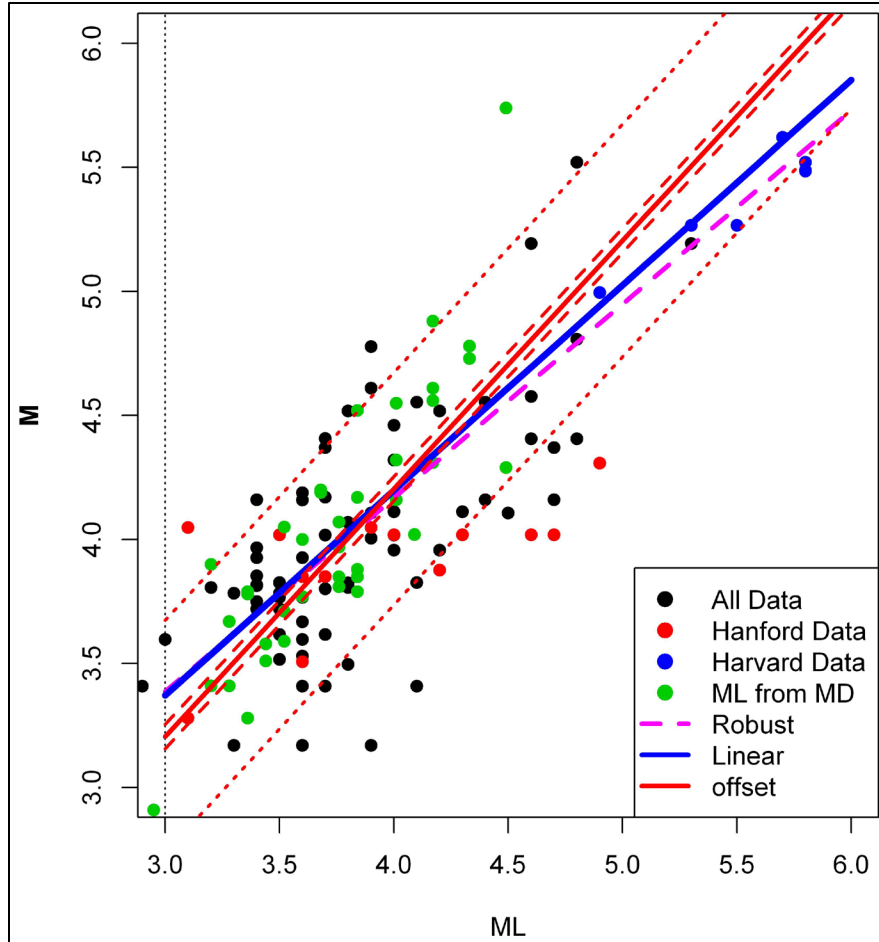


Figure 6.14. Regression of M_L and M .

Equation 6.6 was used to convert the data points shown in green in Figure 6.13 from M_D to M_L . The augmented data set was fitted using three models: an offset model (shown by the red curve), a linear model (shown by the blue curve), and a model using robust regression (purple curve). The figure also shows the conversion equation based on Utsu (2002) that is used in the U.S. National Seismic Hazard Maps (C. Mueller, email communication to Valentina Montaldo-Falero and Bob Youngs, dated June 12, 2013). Three information criteria (AIC, AICc, and BIC) were applied to guide the selection of the best-fitting model, which was found to be the linear model. The conversion equation is as follows:

$$E[\mathbf{M}] = 0.89 + 0.83 M_L \quad (6.7)$$

$$\sigma_{\mathbf{M}|M_L} = 0.31$$

Following NUREG-2115, $\sigma_{\mathbf{M}|M_L}$ is calculated as the difference between the sigma of 0.27 obtained from the regression, increased by the variance of the M_L obtained from M_D (normalized by the number of data), and reduced by the average value of $\sigma[\mathbf{M}|\hat{\mathbf{M}}] = 0.12$ for the earthquakes used in this regression.

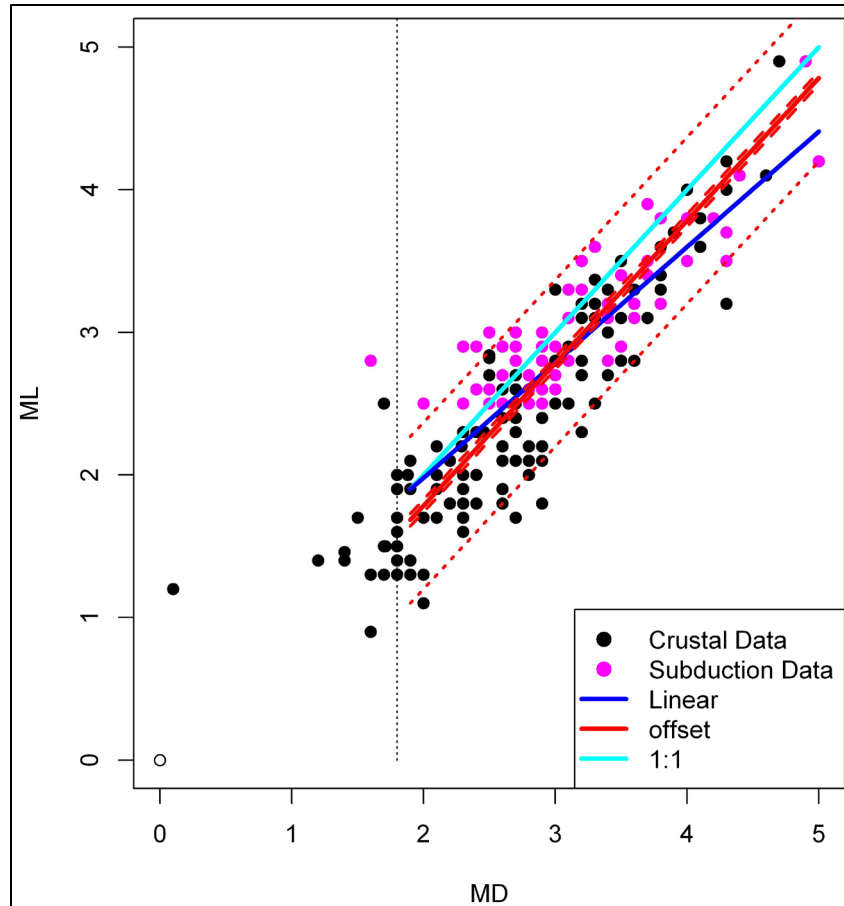


Figure 6.15. Regression of M_L and M_D .

6.5.3 Conversion from Macroseismic Intensities

The crustal earthquake catalog contains 107 earthquakes with at least one instrumental magnitude and a measure of maximum macroseismic intensity (I_0), almost half of which are obtained from the USGS “Did You Feel It?” website. It should be noted that these intensities are generally small, $MMI \leq IV$, and sometimes based on few and sparse responses.

The first step in the analysis of the data set was to eliminate all pre-1969 earthquakes with an instrumental magnitude equal to the MI (magnitude from intensity) obtained using the Gutenberg formula ($MI = 2/3 I_0 + 1$). Then, the data were inspected to identify correlations with different instrumental magnitudes; Figure 6.16 shows the correlation between I_0 and M , M_D , or M_S . The red curve in Figure 6.16b and c is the Gutenberg relation. As mentioned in Section 6.2.5, the Rossi-Forel intensities have been converted to MMIs using the approximate conversion from Richter (1958).

The I_0 - M_D data set shown in Figure 6.16b covers the lower intensities, while the I_0 - M_S data set shown in Figure 6.16c expands the data range to higher intensities. Because there are not many data with I_0 and M in the catalog database, the data set was augmented by converting M_D and M_S to $E[M]$ using Equations 6.4 and 6.5. For each earthquake in the data set that contains M and another instrumental magnitude, preference is given to M ; if an earthquake has M_D and M_S but no M , preference is given to $E[M|M_S]$.

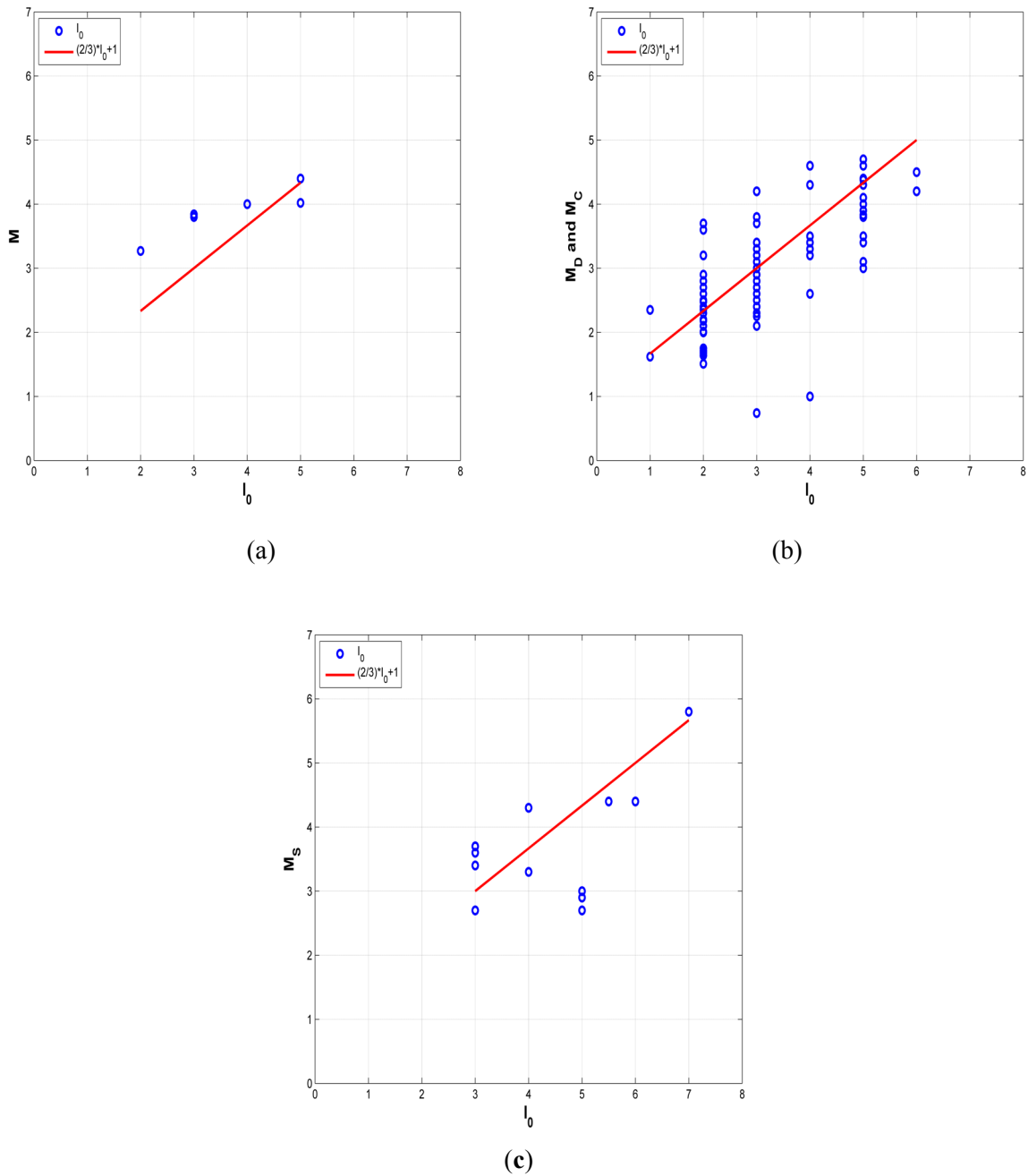


Figure 6.16. Relationships between (a) I_0 vs M ; (b) I_0 vs M_D ; (c) I_0 vs M_S .

The three largest intensities in the data set used for regression analysis are MMI VI obtained from the “Did You Feel It?” website (USGS 2013a) for an earthquake that occurred in Montana on July 26, 2005, MMI VII for the July 3, 1999 earthquake in Washington, and MMI VIII for the February 28, 2001 Nisqually earthquake in Washington. These intensities were obtained from the USGS webpage on significant earthquakes in the state of Washington (USGS 2013a, b).

NUREG-2115 shows that a linear relationship between I_0 and M is appropriate for intensity data greater than IV. The data set shown in Figure 6.15 was trimmed at MMI IV, which eliminates most of the “Did You Feel It?” data points, and truncated at M 2; then a linear model was fitted through the data (purple curve in Figure 6.17). A locally weighted least-squares fit (Loess) to the data confirms that the linear fit is appropriate in this intensity range (blue curve in Figure 6.17). The linear model is very similar to the Loess model for MMI up to VI-VII, and produces lower $E[M]$ for $MMI \leq VII$ than the Gutenberg relation, which is shown for comparison by the green curve. The linear model is given in Equation 6.8:

$$E[M|I_0] = 0.27 + 0.75 I_0 \tag{6.8}$$

$$\sigma_{M|I_0} = 0.50$$

where $\sigma_{M|I_0}$ is calculated from the regression sigma of 0.46 and the variance of the $E[M]$ obtained from the observed M , M_S , M_D and the appropriate conversions. Equation 6.8 is considered applicable to the subduction and crustal catalogs for $MMI \geq IV$.

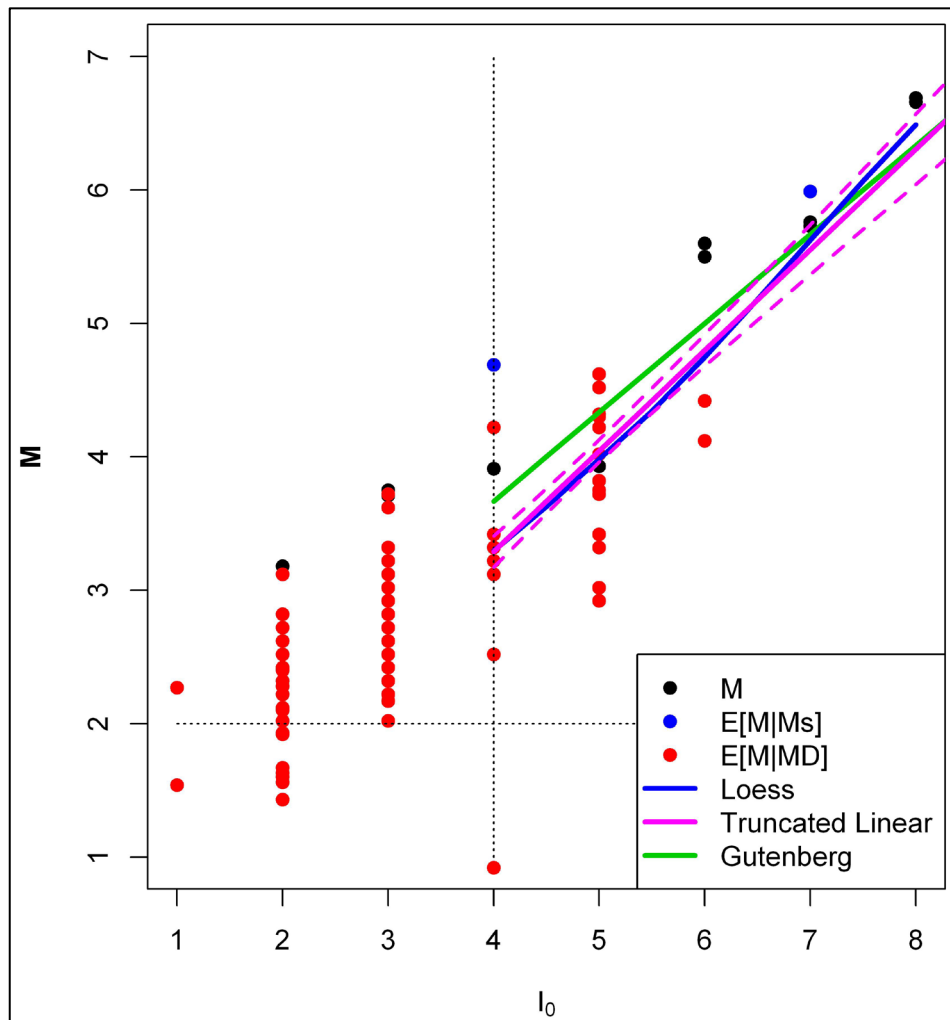


Figure 6.17. Regression between I_0 and M .

6.5.4 Treatment of Magnitude Uncertainties in Recurrence Calculations

Earthquake magnitudes are calculated as a statistical average of measurements obtained at a number of seismic stations, and although it is typically not reported in the earthquake catalogs, a certain amount of uncertainty is associated with each reported magnitude. Additional uncertainty is then introduced by using magnitude conversion relations. This uncertainty is symmetrically distributed around the magnitude value. The standard approach to calculating recurrence rates is to obtain earthquake counts for magnitude bins. Gutenberg and Richter (1944) demonstrate that, in a large region, earthquake magnitudes follow an exponential distribution; that is, the earthquake magnitude bin m_i contains more earthquakes than in the next larger magnitude bin m_{i+1} . The unequal number of earthquakes in adjacent magnitude bins means that more earthquakes are shifted from magnitude bin m_i to the next larger magnitude bin m_{i+1} than from m_{i+1} to m_i due to the statistical magnitude uncertainty. This bias was studied independently by Tinti and Mulargia (1985) and by EPRI/SOG (1988). Each study proposed an approach to correct the bias: the Tinti and Mulargia (1985) approach is to correct the earthquake counts; the EPRI/SOG (1988) approach is to correct the magnitudes (M^* approach). More recently, NUREG-2115 addressed the bias by adopting the Tinti and Mulargia (1985) approach to correct the earthquake counts, but applied to each individual earthquake rather than to the total earthquake counts within a magnitude bin. The NUREG-2115 approach is called the N^* approach and allows for maintaining the EPRI/SOG (1988) ability to account for differences in magnitude uncertainty for individual earthquakes. Statistical tests described in NUREG-2115 show that for a catalog with variable levels of completeness, such as the Hanford crustal and subduction catalogs, the N^* approach performs better than the M^* approach, therefore the N^* approach is followed in this study.

The N^* approach can be described as follows:

1. The earthquake catalog is processed to obtain values of $E[\mathbf{M}]$ and $\sigma[\mathbf{M}]$ for each earthquake using the following equations (from EPRI/SOG 1988):

$$E[\mathbf{M} | \hat{\mathbf{X}}] = \left\{ \sum_i \frac{\sigma^2[\mathbf{M} | \hat{\mathbf{X}}]}{\sigma^2[\mathbf{M} | \hat{\mathbf{X}}_i]} \cdot E[\mathbf{M} | \hat{\mathbf{X}}_i] \right\} + (R-1)\beta\sigma^2[\mathbf{M} | \hat{\mathbf{X}}] \quad (6.9)$$

and

$$\sigma^2[\mathbf{M} | \hat{\mathbf{X}}] = \left\{ \sum_i \frac{1}{\sigma^2[\mathbf{M} | \hat{\mathbf{X}}_i]} \right\}^{-1} \quad (6.10)$$

where $\hat{\mathbf{X}}_i$ is a single member of $\hat{\mathbf{X}}$.

2. Each earthquake is then assigned an equivalent count N^* defined in NUREG-2115 as follows:

$$N^* = \exp\left\{\beta^2 \sigma^2 [|\mathbf{M}| \hat{\mathbf{M}}] / 2\right\}$$

or

$$N^* = \exp\left\{\beta^2 \sigma^2 [|\mathbf{M}| \mathbf{X}] / 2\right\} \tag{6.11}$$

where $\hat{\mathbf{M}}$ is the observed moment magnitude. N^* accounts for the uncertainty in the magnitude of each earthquake by including the variance calculated in Equation 6.10.

3. The earthquake rates are computed by summing the effective counts N^* within each magnitude bin and dividing it by the period of completeness for that magnitude bin.

6.5.5 Uniform Moment Magnitude Catalog of $E[\mathbf{M}]$ and N^* Values

The conversion equations listed in the previous sections were used to convert the available magnitude estimates to a uniform value of the expected moment magnitude ($E[\mathbf{M}]$). For earthquakes with an observed \mathbf{M} obtained from the seismic moment, $E[\mathbf{M}]$ is calculated exclusively from this value, based on the assumption that an observed \mathbf{M} should be preferred to other size measures. Other types of moment magnitude (e.g., M_w reported in a catalog without an associated seismic moment) are combined with all other available magnitude types. Values of $E[\mathbf{M}]$, $\sigma[\mathbf{M}]$, and N^* for each earthquake are calculated with Equations 6.9, 6.10, and 6.11 and can be found in Appendix, Sections C.1 (crustal catalog) and C.2 (subduction catalogs).

Figure 6.18 shows the crustal catalog with uniform $E[\mathbf{M}]$, and Figure 6.19 and Figure 6.20 show the two subduction catalogs converted to $E[\mathbf{M}]$ (see Section 10.2.2.2.1 for a discussion of the sensitivity of the seismic hazard to alternative catalogs). The limits of applicability of the conversion relations determine a minimum $E[\mathbf{M}]$ of 1.85 in all catalogs; the maximum $E[\mathbf{M}]$ in the crustal catalog is 7.06 for the 1872 Chelan earthquake and the maximum $E[\mathbf{M}]$ in the subduction catalogs is 6.8 for the 2001 Nisqually earthquake. Unless indicated otherwise, all magnitudes shown in seismicity maps and plots in this report are $E[\mathbf{M}]$ and the minimum magnitude is 1.85.

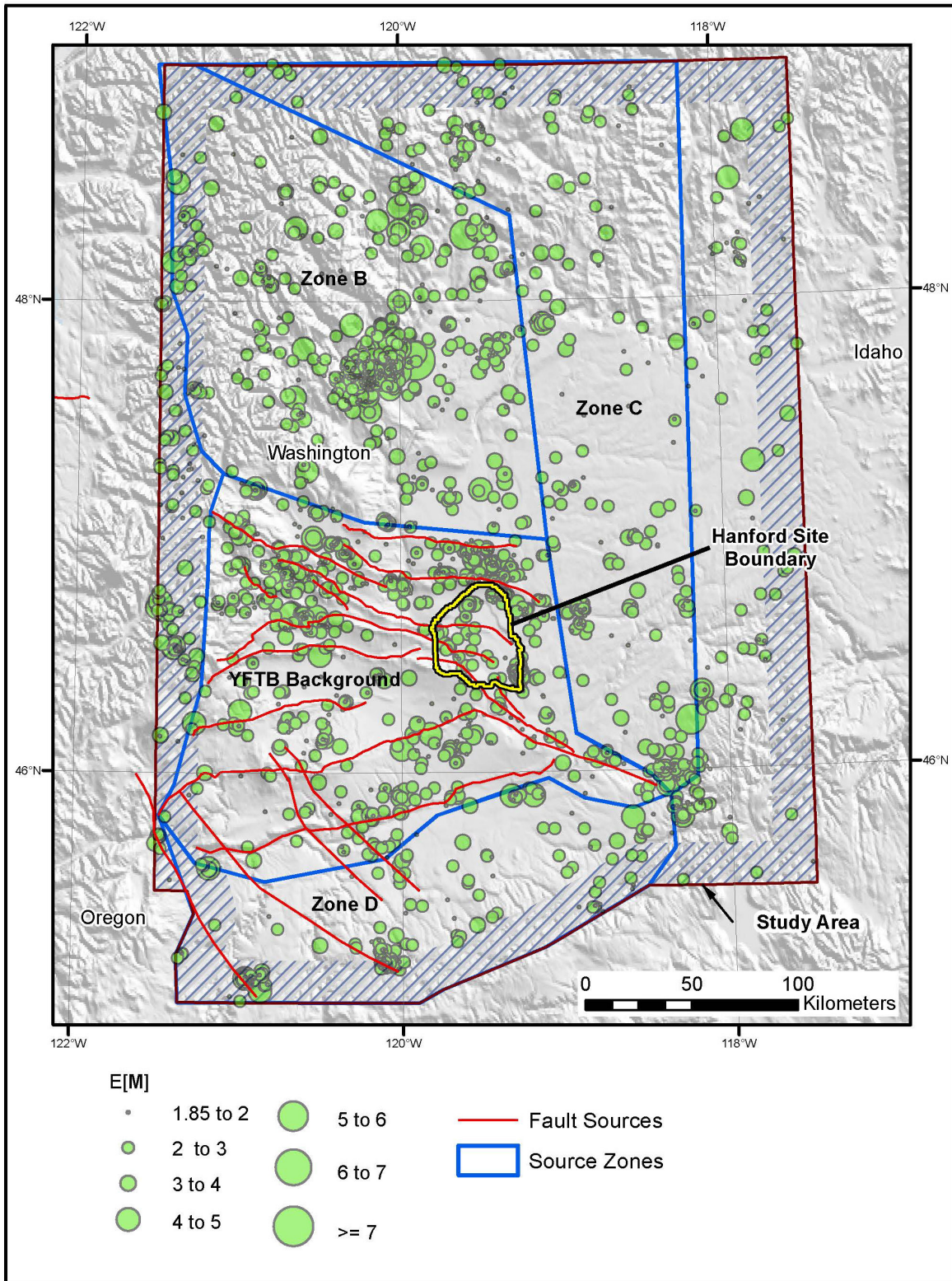


Figure 6.18. Map of the crustal earthquake catalog with magnitudes given in E[M].

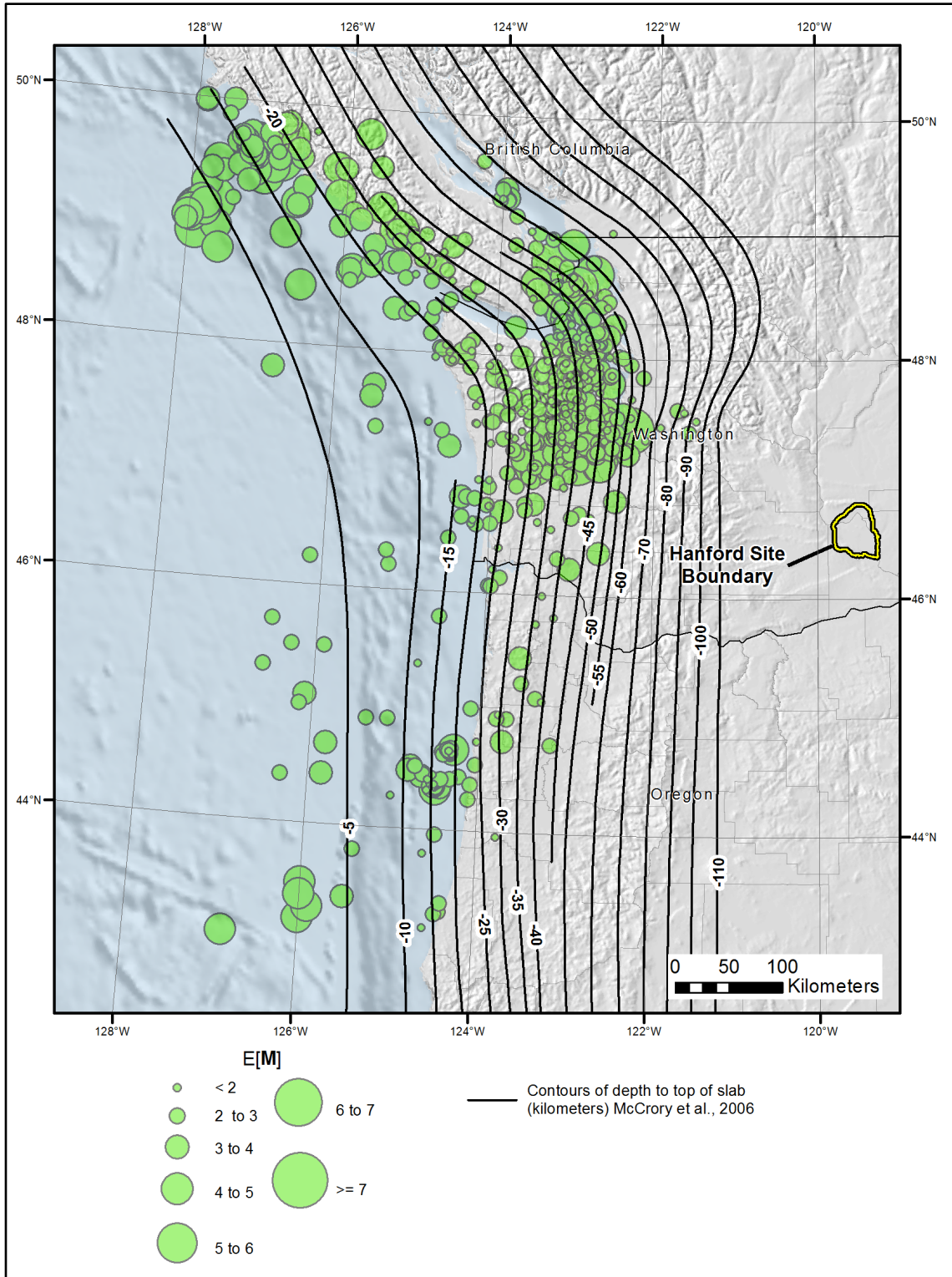


Figure 6.19. Map of the subduction earthquake catalog in E[M].

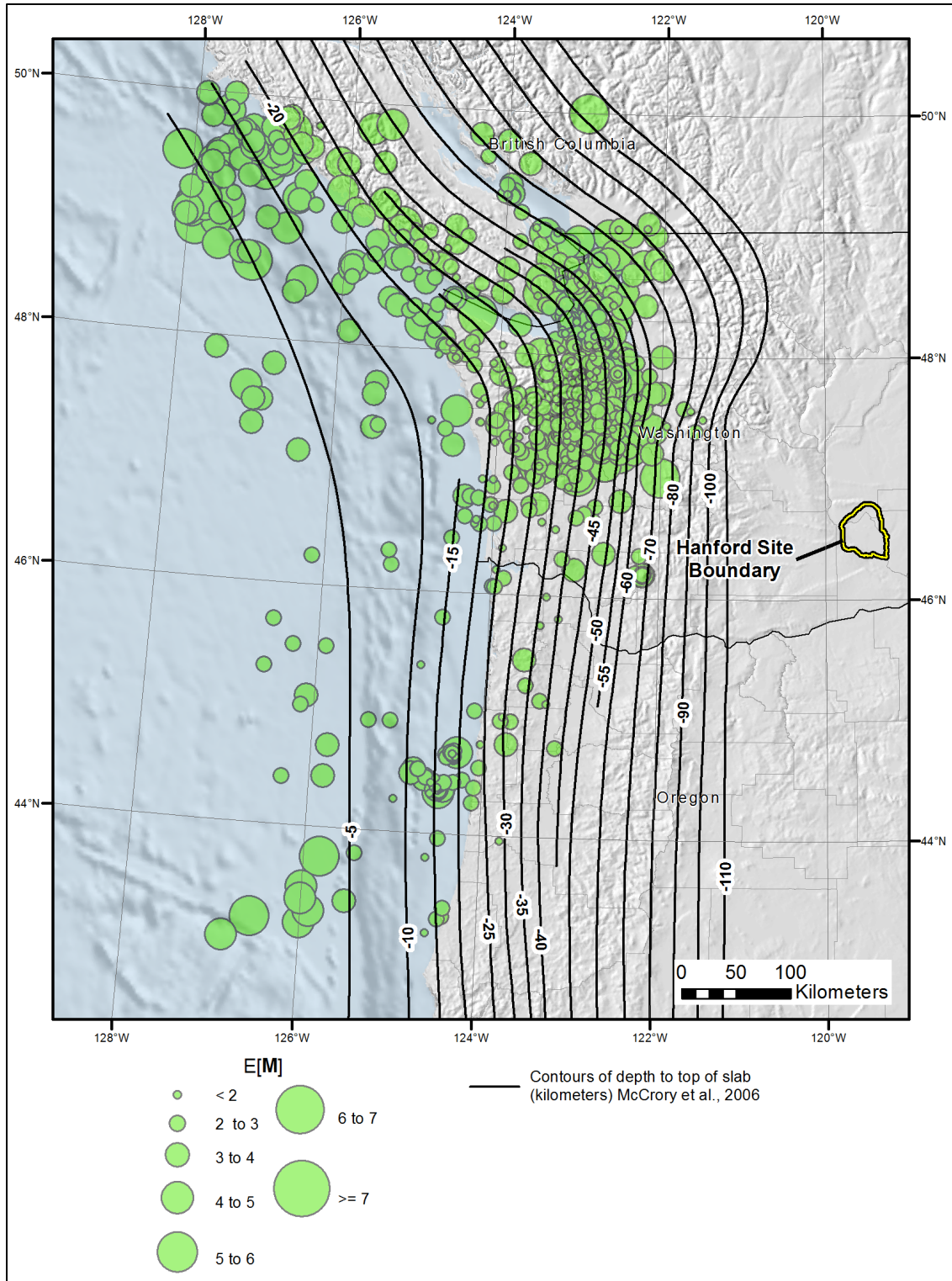


Figure 6.20. Map of the subduction earthquake catalog in E[M] including earthquakes with unknown depths.

6.6 Declustering of the Earthquake Catalogs

Earthquake catalogs typically contain a combination of foreshocks, mainshocks, and aftershocks. In standard PSHA, the mainshocks are assumed to follow a Poisson model in time and are used to estimate the frequency of earthquakes within a source zone. The occurrence of aftershocks, instead, follows the Omori law that predicts the evolution of the aftershock sequence as a function of the magnitude of the mainshock.

The process of identifying and removing aftershocks and foreshocks is called earthquake declustering and various techniques exist that perform this operation. These techniques are typically based on the use of fixed time and distance windows or on the use of statistical analysis.

6.6.1 Alternative Declustering Approaches

Gardner and Knopoff (1974) were the first to develop time and distance windows as a function of earthquake magnitude to use in identifying dependent earthquakes. For each large earthquake, the method defines a fixed time window and a fixed distance window whose length is dependent on the magnitude of the large earthquake (mainshock). Every smaller earthquake that occurred within those windows is considered a dependent earthquake. The Gardner and Knopoff (1974) method was originally derived using a catalog of earthquakes in southern California, but has since been applied to other regions, and alternative time and distance windows have been introduced. For the Hanford PSHA project, the Gardner and Knopoff (1974) method and two of its modifications, by Grünthal (1985) and Uhrhammer (1986), were used.

The fourth method used to decluster the Hanford catalogs was developed by EPRI/SOG (1988, Vol. 1) and involves the use of statistical testing to identify clusters of earthquakes. The earthquake catalog is ordered from the largest to the smallest earthquake, then the algorithm constructs a local space-time window in the immediate vicinity of the selected earthquake, and a much larger extended window. The null hypothesis used by the algorithm is that, assuming a Poisson process, the seismicity should not be elevated within the local window. If the null hypothesis is rejected, the algorithm keeps testing adjacent space and time windows until none is found that rejects the null hypothesis. The final step in the process is to reduce the earthquake counts in the cluster region to match the background rate in the extended window. The process is repeated a second time, after removing all of the events identified as secondary during the first step. As discussed in NUREG-2115, the advantages of the EPRI/SOG (1988) approach are that it is insensitive to incompleteness because a homogeneous Poisson process is only assumed in proximity to the earthquake sequence being tested and that it does not assume a priori a shape for the clusters.

Recently, Jacobs et al. (2013) proposed a method that uses changes in the cumulative earthquake rate to identify earthquake clusters (cumulative rate analysis [CURATE] method). CURATE was developed in particular for earthquake catalogs containing swarms, which are often characterized by very long durations and the lack of a mainshock. The application of the method involves a number of steps, the first being to check for temporal relationships between earthquakes. This is done by calculating the expected cumulative number of earthquakes in the catalog and comparing that number with the observed number. Deviations from the expected number are used to identify potential sequences. The second step is to apply a distance rule to check for a spatial correlation of the earthquakes within each preliminary

sequence. The method also addresses the issue of linkage between earthquake sequences by allowing sequences occurring in the same location within a certain number of days to be related. An application of the method to a catalog of earthquakes in the Central Volcanic Region of New Zealand shows that results are consistent with those obtained by other standard declustering techniques.

Within the framework of the NGA-West2 (Next Generation Attenuation Relationships for the Western United States) project sponsored by the Pacific Earthquake Engineering Research Center (Bozorgnia et al. 2014), a common declustering technique was applied to separate the earthquakes in the NGA database between two categories called Class 1 and Class 2. The definition given by Wooddell and Abrahamson (2012) is that Class 1 earthquakes are mainshocks, triggered events, or foreshocks that occur off the surface projection of the mainshock rupture plane, and Class 2 earthquakes are the earthquakes that occur within or near the surface projection of the mainshock rupture plane and within a time window for aftershocks. This definition is important for developing ground motion predictive relationships because it has been observed that Class 2 earthquakes tend to produce lower median ground motions than Class 1 earthquakes of the same magnitudes because their stress drop is lower. The declustering algorithm adopted in the NGA-West2 project uses the Gardner and Knopoff (1974) fixed time windows and computes a distance window based on the shortest distance between the centroid of Joyner-Boore rupture surface of the Class 2 earthquakes, and the closest point on the edge of the Joyner-Boore rupture surface of the Class 1 mainshock (called the Centroid Joyner-Boore Distance). Wooddell and Abrahamson (2012) applied this method to the Wenchuan, China, earthquake and showed that the direct application of the Gardner and Knopoff (1974) technique misclassifies a large number of aftershocks because the fixed distance window is much smaller than the earthquake rupture.

6.6.2 Application to Hanford PSHA Project Catalog

For the Hanford PSHA project, four alternative techniques were used to identify independent events: three are based on the use of fixed time and distance windows (Gardner and Knopoff 1974; Grünthal 1985; Uhrhammer 1986), and the EPRI/SOG (1988) method is based on statistical testing of clusters of earthquakes.

The method by Jacobs et al. (2013) was considered for application in the YFB where earthquake swarms are known to occur. The CURATE method, however, was not applied because the authors did not provide the project with an algorithm in the time frame required to perform the analyses. The declustering algorithm used in the NGA-West2 project is an improvement of the Gardner and Knopoff (1974) methodology as far as the distance dependence between aftershocks and mainshocks is concerned. As illustrated in the previous section and in the example offered by Wooddell and Abrahamson (2012), the use of the Centroid Joyner-Boore Distance represents an improvement only for large earthquakes that have very long rupture lengths. This is not the case for most earthquakes in the Hanford catalogs. Moreover, the method requires knowledge of the rupture plane, which is also not available for the majority of the earthquakes in the Hanford catalogs. Finally, the method does not address the time dependency of aftershock and mainshock, which is a key element in the evaluation of earthquake recurrence, but adopts the Gardner and Knopoff (1974) windows.

The crustal and subduction catalogs were declustered using the four methods listed above. Results are shown in Table 6.3, which compares the number of earthquakes inside the magnitude bins used in recurrence calculations obtained from each of the declustered catalog. As expected, the methods differ

Table 6.3. Number of earthquakes per magnitude bin from the declustered crustal catalogs and the declustered subduction catalogs.

E[M] Interval	Before Declustering	Grünthal (1985)	Gardner & Knopoff (1974)	Uhrhammer (1986)	EPRI/SOG (1988, Vol. 1)
Completeness Region North					
2.00 to 2.50	1741	1165	1332	1547	1211
2.50 to 3.00	338	236	272	305	261
3.00 to 3.50	170	131	143	151	133
3.50 to 4.00	60	46	53	57	51
4.00 to 4.50	61	46	48	51	50
4.50 to 5.00	11	10	10	10	10
5.00 to 5.75	1	1	1	1	1
5.75 to 6.50	1	1	1	1	1
>6.50	1	1	1	1	1
Completeness Region South					
2.00 to 2.50	300	261	275	289	275
2.50 to 3.00	106	83	91	97	94
3.00 to 3.50	74	62	61	67	64
3.50 to 4.00	63	43	47	51	48
4.00 to 4.50	31	16	18	19	19
4.50 to 5.00	26	17	17	19	19
5.00 to 5.75	6	5	6	6	6
5.75 to 6.50	10	9	9	9	9
>6.50	3	3	3	3	3
Completeness Region for Subduction					
2.00 to 2.50	306	266	280	295	280
2.50 to 3.00	120	91	101	108	111
3.00 to 3.50	117	94	96	108	101
3.50 to 4.00	103	74	79	89	82
4.00 to 4.50	53	37	40	42	42
4.50 to 5.00	45	32	35	37	34
5.00 to 5.75	14	12	13	14	13
5.75 to 6.50	11	10	10	10	6
>6.50	3	3	3	3	2

primarily for small magnitudes (less than E[M] 4); the method by Grünthal (1985) consistently removes more earthquakes than the other three methods, and the method by Uhrhammer (1986) consistently removes fewer earthquakes than the other methods. The remaining two methods (EPRI-SOG and Gardner and Knopoff) produce similar results, with differences in the overall number of independent earthquakes ranging between 2 percent or less for the subduction catalogs and 6 percent for the crustal catalog. A similar comparison is documented in NUREG-2115 for the Central and Eastern United States catalog, where differences between the two methodologies produced a 1.5 percent difference in the overall number of independent earthquakes, with a maximum of 4.4 percent in the E[M] 2.9 to 3.6 magnitude bin.

6.7 Catalog Completeness

The procedure to calculate earthquake recurrence rates requires an assessment of the time periods over which independent earthquakes have been completely recorded in the earthquake catalog. In standard PSHAs there are two approaches to the assessment of catalog completeness: one is the method originally proposed by Stepp (1972) and the other is based on the concept of probability of detection, which was introduced by Veneziano and Van Dyck (1985) and evolved in the methodology used in the EPRI/SOG (1988) project (and subsequently in NUREG-2115). The two methods are described in the following sections.

6.7.1 The Stepp Method

The Stepp (1972) method defines the completeness for a specific magnitude range by counting the total number of earthquakes in the catalog within that magnitude range, starting from present and moving back in time. Every time an earthquake of that magnitude occurred, the rate was calculated by dividing the number of earthquakes counted from present to that point in time by the corresponding time interval (from present to that point in time). The assumption made in the PSHA is that earthquakes follow a stationary Poisson process in time, so the rate of earthquakes when plotted as a function of time should show a nearly horizontal trend for the complete portion of the catalog, and a downward trending slope for the incomplete part. The point in time where the slope begins is considered the beginning of the complete period.

It is common practice in the PSHA to use only the earthquakes that occurred in the complete portion of the catalog for calculating earthquake recurrence parameters. Earthquake rates are calculated by counting the number of earthquakes within each magnitude bin and completeness time interval and dividing the counts by the length of the complete time interval. Veneziano and Van Dyck (1985) define an equivalent period of completeness (TE) such that the rate of earthquake occurrence is equal to the total number of events in the catalog within a given magnitude range, divided by TE . The method is based on the assessment of the probability of detection (P^D) as a function of magnitude, time, and completeness region. Under the assumption that seismicity in a region follows a stationary Poisson process in time, the rate of observed earthquakes v_i for magnitude interval m_{i-1} to m_i is given by

$$v_i = \lambda_i P_i^D(t) \quad (6.12)$$

where λ_i is the true rate of earthquakes in the specified magnitude interval, and $P_i^D(t)$ is the probability of detection of earthquakes in that magnitude bin as a function of time. If the entire length of the catalog is subdivided into J time periods such that within each j period the probability of detection can be assumed to be relatively constant, the probability of observing the recorded number of earthquakes (n_{ij}) is given by the Poisson distribution

$$P(N = n_{ij}) = \frac{(v_i t_j)^{n_{ij}} e^{-v_i t_j}}{n_{ij}!} \quad (6.13)$$

Combining Equations 6.12 and 6.13, the likelihood of observing the recorded earthquakes in the magnitude interval m_{i-1} to m_i is given by

$$L(\lambda_i, P_{ij}) = \prod_{j=1}^J \frac{(\lambda_i t_j P_{ij})^{n_{ij}} e^{-\lambda_i t_j P_{ij}}}{n_{ij}!} \quad (6.14)$$

where P_{ij} is the probability of detection of events in the i -th magnitude interval in the time period j . If it is assumed that the larger magnitudes are complete at present and that P^D should decrease monotonically from the present time, Equation 6.11 can be maximized to obtain the parameters most likely to represent the Poisson process that produces the observed earthquake catalog. The equivalent time of completeness TE is given by

$$TE_i = \sum_{j=1}^J P_{ij} t_j \quad (6.15)$$

6.7.2 Probability of Detection in Space and Time

The assessment of catalog completeness requires the delineation of completeness regions. The subduction catalog is analyzed using only one completeness region, whereas the area covered by the Hanford crustal catalog is subdivided into two zones: a southern region that covers the YFB, and a northern region that includes the concentration of seismicity around Lake Chelan. Tests were conducted to see whether the seismicity around Lake Chelan should be kept in a separate completeness region; the results indicated that the probabilities of detection for the Lake Chelan area are not significantly different from the probabilities of detection for the northern region, particularly for large magnitudes.

For each earthquake catalog a standard evaluation of completeness with Stepp plots was used to estimate the time intervals (t_j in Equations 6.10 through 6.13) within which the probability of detection can be assumed to be relatively constant. These periods are 1850 to 1890, 1891 to 1930, 1931 to 1950, 1951 to 1970, 1971 to 1980, and 1981 to present for the crustal catalog, and 1850 to 1900, 1901 to 1930, 1931 to 1950, 1951 to 1970, 1971 to 1980, and 1981 to present for the subduction catalog. Because the Hanford earthquake catalogs, particularly the crustal catalog, do not contain very many earthquakes of moderate to large magnitude, defining completeness based on the Stepp plots is difficult. The use of probability of detection is the preferred approach because it allows for the inclusion of earthquakes that occurred in the incomplete portion of the earthquake catalog.

The algorithm for the calculation of probability of detection and equivalent time of completeness requires an initial guess of the probability of detection for each magnitude and time interval (P_{ij}^D). The installation of the PNSN in 1969 marks a clear change in the recording capability in the Pacific Northwest, prior to which there are only sparse instrumental recordings of earthquakes occurred since the 1930s. Based on this information, together with the history of settlement in Washington and particularly along the Columbia River, the probability of detection for the larger magnitude earthquakes is 1 at least through the 1930s, and decreases monotonically in time before that. The probability of detection of smaller magnitude earthquakes ($E[M] 3$ to 3.5) is initially set to 1 since the installation of the PNSN.

Table 6.4 shows the resulting probabilities of detection subdivided by completeness region, magnitude and time interval, and the corresponding equivalent time of completeness for use in earthquake recurrence analyses.

Table 6.4. P^D and equivalent time of completeness by completeness region, magnitude and time intervals, and catalog.

Completeness Region North							
E[M] interval	1866 to 1890	1890 to 1930	1930 to 1950	1950 to 1970	1970 to 1980	1980 to 2013	TE
2.00 to 2.50	0.00	0.00	0.00	0.01	0.10	0.18	7.11
2.50 to 3.00	0.00	0.00	0.00	0.05	0.26	0.49	19.70
3.00 to 3.50	0.00	0.06	0.38	0.38	0.42	0.84	49.58
3.50 to 4.00	0.00	0.19	0.89	0.90	1.00	1.00	86.51
4.00 to 4.50	0.00	0.99	1.00	1.00	1.00	1.00	122.64
4.50 to 5.00	0.00	0.99	1.00	1.00	1.00	1.00	122.74
5.00 to 5.75	0.00	1.00	1.00	1.00	1.00	1.00	122.82
5.75 to 6.50	0.01	1.00	1.00	1.00	1.00	1.00	123.23
>6.50	1.00	1.00	1.00	1.00	1.00	1.00	146.89
Completeness Region South							
E[M] interval	1866 to 1890	1890 to 1930	1930 to 1950	1950 to 1970	1970 to 1980	1980 to 2013	TE
2.00 to 2.50	0.00	0.00	0.01	0.04	0.60	0.67	29.18
2.50 to 3.00	0.00	0.00	0.04	0.15	0.75	0.83	38.80
3.00 to 3.50	0.02	0.02	0.13	0.54	0.90	1.00	56.41
3.50 to 4.00	0.14	0.14	0.24	0.91	0.91	1.00	74.19
4.00 to 4.50	0.24	0.24	0.24	0.91	0.91	1.00	80.62
4.50 to 5.00	0.39	0.39	0.39	0.92	0.92	1.00	93.00
5.00 to 5.75	0.39	0.39	0.39	1.00	1.00	1.00	95.70
5.75 to 6.50	0.42	0.42	0.42	1.00	1.00	1.00	98.55
>6.50	0.43	0.43	0.43	1.00	1.00	1.00	98.97
Completeness Region for Subduction							
E[M] interval	N/A	1900 to 1930	1930 to 1950	1950 to 1970	1970 to 1980	1980 to 2013	TE
3.00 to 3.50	--	0.00	0.00	0.12	0.68	0.71	32.66
3.50 to 4.00	--	0.00	0.00	0.17	0.77	1.00	44.06
4.00 to 4.50	--	0.00	0.16	0.77	1.00	1.00	61.59
4.50 to 5.00	--	0.00	0.16	1.00	1.00	1.00	66.24
5.00 to 5.75	--	0.99	1.00	1.00	1.00	1.00	112.82
5.75 to 6.50	--	1.00	1.00	1.00	1.00	1.00	112.96
>6.50	--	1.00	1.00	1.00	1.00	1.00	113.00
Completeness for Subduction (including unknown depths in the catalog)							
E[M] interval	1800 to 1900	1900 to 1930	1930 to 1950	1950 to 1970	1970 to 1980	1980 to 2013	TE
3.00 to 3.50	0.00	0.01	0.01	0.47	0.57	0.73	39.65
3.50 to 4.00	0.00	0.01	0.01	0.80	1.00	1.00	59.67
4.00 to 4.50	0.10	0.57	0.80	0.99	1.00	1.00	105.44
4.50 to 5.00	0.32	0.91	0.99	1.00	1.00	1.00	142.21
5.00 to 5.75	0.85	0.92	1.00	1.00	1.00	1.00	195.55
5.75 to 6.50	0.85	0.92	1.00	1.00	1.00	1.00	196.23
>6.50	0.92	1.00	1.00	1.00	1.00	1.00	205.46

6.8 References

- ANSS (Advanced National Seismic System). 2013. Catalog available at: <http://www.quake.geo.berkeley.edu/anss/catalog-search.html>; accessed May 3, 2013.
- Bakun WH, RA Haugerud, MG Hopper, and RS Ludwin. 2002. The December 1872 Washington State Earthquake. *Bulletin of the Seismological Society of America* 92(8):3239–3258.
- Bozorgnia Y, NA Abrahamson, LA Atik, and 30 other authors. 2014. NGA-West2 Research Project. *Earthquake Spectra*, 30(3): 973-987.
- Crider JG, RS Crosson, and J Brooks. 2003. The Chelan Seismic Zone, the Great Terrace and the December 1872 Washington State Earthquake. *Geological Society of America Abstracts with Programs* 35:645.
- EPRI/SOG (Electric Power Research Institute Seismic Owners Group). 1988. *Seismic Hazard Methodology for the Central and Eastern United States*. Technical Report NP-4726-A, Volumes 1–10, EPRI, Palo Alto, California.
- Foxall B and T Turcotte. 1979. Seismological investigation of the Walla Walla/Milton-Freewater area (abstract). *Earthquake Notes* 50:7.
- Gardner JK and L Knopoff. 1974. Is the sequence of earthquakes in Southern California, with aftershocks removed, Poissonian? *Bulletin of the Seismological Society of America* 64(5):1363–1367.
- Geomatrix (Geomatrix Consultants, Inc.). 1995. *Seismic Design Mapping, State of Oregon*. Final Report prepared for the Oregon Department of Transportation, Personal Services Contract 11688, 11 plates. Geomatrix Consultants, Inc., San Francisco, California.
- Gomberg J, B Sherrod, M Trautman, E Burns, and D Snyder. 2012. Contemporary Seismicity in and around the Yakima Fold-and-Thrust Belt in Eastern Washington. *Bulletin of the Seismological Society of America* 102(1):309–320. DOI: 10.1785/0120110065.
- Grünthal G. 1985. The up-dated earthquake catalogue for the German Democratic Republic and adjacent areas—Statistical data characteristics and conclusions for hazard assessment. In *Proceedings of the 3rd International Symposium on the Analysis of Seismicity and Seismic Risk*, Liblice Castle, Czechoslovakia, June 17-22, 19-25. Geophysical Institute of the Czechoslovak Academy of Sciences, Prague, Czech Republic.
- Gutenberg B and C Richter. 1944. Frequency of earthquakes in California. *Bulletin of the Seismological Society of America* 34:185–188.
- Halchuck S. 2009. *Seismic Hazard Epicenter File (SHEEF) Used in the Fourth Generation Seismic Hazard Maps of Canada*. Geological Survey of Canada, Open File 6208, 1 CD-ROM. Ottawa, Canada.
- Hanks TC and H Kanamori. 1979. A moment-magnitude scale. *Journal of Geophysical Research* 84:2348–2350.

HCMT (Harvard Centroid Moment Tensor) catalog. 2013. Available at: <http://www.globalcmt.org/CMTsearch.html>. Accessed on June 25, 2013.

ISC (International Seismological Centre). 2013. Available at: <http://www.isc.ac.uk/iscbulletin/search/catalogue/>. Accessed on May 13, 2013.

Jacobs KM, EGC Smith, MK Savage, and J Zhuang. 2013. Cumulative rate analysis (CURATE): A clustering algorithm for swarm dominated catalogs. *Journal of Geophysical Research: Solid Earth* 118(2): 553–569. DOI: 10.1029/2012JB009222.

JBA (Jack Benjamin & Associates), URS Corporation Seismic Hazards Group, Geomatrix Consultants, Inc., and Shannon & Wilson. 2012. *Probabilistic Seismic Hazard Analyses Project for the Mid-Columbia Dams*. Final Report prepared for the Public Utility Districts of Chelan, Douglas, and Grant Counties. Chelan County PUD, Wenatchee, Washington

Ludwin R. 2006. *Cascadia Historic Earthquake Catalog, 1793-1929 Covering Washington, Oregon and Southern British Columbia*. Provided by The Pacific Northwest Seismic Network. Available at: https://old.pnsn.org/HIST_CAT/CASCAT2006/about.html; accessed on May 10, 2013.

Ludwin RS, CS Weaver, and RS Crosson. 1991. Seismicity of Washington and Oregon. Chapter 6 in *Neotectonics of North America – The Geology of North America Decade Map Volume 1*, DB Slemmons, ER Engdahl, MD Zoback, and DD Blackwell (eds.), pp. 77–98. Geological Society of America, Boulder, Colorado.

Mann GM and CE Meyer. 1993. Late Cenozoic structure and correlations to seismicity along the Olympic-Wallowa Lineament, northwest United States. *Geological Society of America Bulletin* 105:853–871.

McCrory PA, JK Blair, DH Oppenheimer, and SR Walter. 2006. *Depth to the Juan de Fuca slab beneath the Cascadia subduction margin. A 3-D model for sorting earthquakes*. U.S. Geological Survey, Data Series 91, Version 1.2. Available at: <http://pubs.usgs.gov/ds/91/>.

NEDB (National Earthquake Data Base). 2013. Available at: <http://www.earthquakescanada.nrcan.gc.ca/stdon/NEDB-BNDS/bull-eng.php>. Accessed on May 3, 2013.

NEIC (National Earthquake Information Center). 2013. Available at: <http://earthquake.usgs.gov/earthquakes/eqarchives/epic/>. Accessed on May 9, 2013.

Neumann F. 1938. *United States earthquakes 1936-1940*. U.S. Coast and Geodetic Survey Serial No. 6510, p. 45. The National Archives and Records Administration, College Park, Maryland.

NRC (U.S. Nuclear Regulatory Commission). 2012. *Central and Eastern United States Seismic Source Characterization for Nuclear Facilities Project*. NUREG-2115, Washington, D.C.

Petersen MD, AD Frankel, SC Harmsen, CS Mueller, KM Haller, RL Wheeler, RL Wesson, Y Zeng, OS Boyd, DM Perkins, N Luco, EH Field, CJ Wills, and KS Rukstales. 2008. *Documentation for the 2008 Update of the United States National Seismic Hazard Maps*. U.S. Geological Survey Open-File Report 2008–1128. Available at: <http://pubs.er.usgs.gov/usgspubs/ofr/ofr081128>.

PNSN (Pacific Northwest Seismic Network). 2013. <http://www.pnsn.org/earthquakes/recent>. Accessed on May 17, 2013.

Richter CF. 1958. *Elementary Seismology*. W.H. Freeman and Co., San Francisco.

Rohay A. 1989. *Earthquake Recurrence Rate Estimates for Eastern Washington and the Hanford Site*. PNL-6956, Research Report prepared for the Westinghouse Hanford Company for the U.S. Department of Energy, by Pacific Northwest Laboratory, Richland, Washington.

Saint Louis University. 2013. *Catalog of Moment Tensors for Parts of North America*. Available at: http://www.eas.slu.edu/eqc/eqc_mt/MECH.NA/; accessed on June 3, 2013.

Sipkin SA. 2003. A correction to body-wave magnitude mb based on moment magnitude Mw. *Seismological Research Letters* 74(6):739–742.

Stepp CJ. 1972. Analysis of the completeness of the earthquake sample in the Puget Sound Area and its effect on statistical estimates of earthquake hazard. In *Proceedings of the International Conference on Microzonation* 2:897–910.

Stover CW and JL Coffman. 1993. *Seismicity of the United States 1568-1989 (Revised)*. U.S. Geological Survey Professional Paper 1527. U.S. Government Printing Office, Washington, D.C.

Tinti S. and F Mulargia. 1985. Effects of magnitude uncertainties on estimating the parameters in the Gutenberg-Richter frequency-magnitude law. *Bulletin of the Seismological Society of America* 74:1681–1697.

Uhrhammer RA. 1986. Characteristics of northern and central California seismicity (abs.). *Earthquake Notes* 57:21.

USGS (U.S. Geological Survey). 2013a. “Did you feel it?” Available at: <http://earthquake.usgs.gov/earthquakes/dyfi/>; accessed on May 7, 2013.

USGS (U.S. Geological Survey). 2013b. Significant earthquakes in the state of Washington. Available at: <http://earthquake.usgs.gov/earthquakes/eqarchives/significant/>; accessed on August 5, 2013.

Utsu T. 2002. “Relationships between magnitude scales.” Pages 733–746 in *International Handbook of Earthquake and Engineering Seismology*, Part A, WHK Lee, H Kanamori, PC Jennings and C Kisslinger (eds.). IASPEI Handbook, Academic Press, New York.

Veneziano D and J Van Dyck. 1985. *Analysis of earthquake catalogs for incompleteness and recurrence rates*. Seismic Hazard Methodology for Nuclear Facilities in the Eastern United States, EPRI Research Projects N. P101-29, EPRI/SOG Draft 85-1, v.2, Appendix A-6. Electric Power Research Institute, Palo Alto, California.

WCC (Woodward-Clyde Consultants). 1980. *Seismological review of the July 16, 1936 Milton-Freewater earthquake source region*. Prepared for the Washington Public Power Supply System, Richland, Washington, by WCC, San Francisco, California.

Wooddell KE and NA Abrahamson. 2012. New earthquake classification scheme for mainshocks and aftershocks in the NGA-West2 ground motion prediction equations (GMPEs). In *Proceedings of the 15th World Conference on Earthquake Engineering*, Lisbon, Portugal. Available at: <http://www.nicee.org/wcee/>.